Reactions of Co-ordinated Ligands. Part 27.[1] Formation of η^3-Allyl and σ-Vinyl Complexes by Nucleophilic Attack on Cationic Molybdenum Monoacetylene Complexes. Molecular Structures of $[Mo(CO)(PEt_3)(\eta^3\text{-}anti\text{-}1\text{-}MeC_3H_4)(\eta^5\text{-}C_9H_7)]$ and $[Mo\{P(OMe)_3\}_3\{\sigma\text{-}(E)\text{-}CH{=}CHBu^t\}(\eta\text{-}C_5H_5)]$ *

Stephen R. Allen, Paul K. Baker, Stephen G. Barnes, Martin Bottrill, Michael Green, A. Guy Orpen, and Ian D. Williams
Department of Inorganic Chemistry, University of Bristol, Bristol BS8 1TS
Alan J. Welch
Department of Chemistry, University of Edinburgh, Edinburgh EH9 3JJ

Reaction of $[MoLL^1(\eta\text{-}MeC_2R)A][BF_4]$ [R = Me, Et, or Pr^i; L = L^1 = $P(OMe)_3$; LL^1 = $Ph_2PCH{=}CHPPh_2$; L = PEt_3, L^1 = CO; A = $\eta\text{-}C_5H_5$ or $\eta^5\text{-}C_9H_7$] with $NaBH_4$ or $K[BHBu^s{}_3]$ in tetrahydrofuran affords the *anti*-substituted η^3-allyl complexes $[MoLL^1(\eta^3\text{-}CH_2\overset{...}{-}CH\overset{...}{-}CHR)A]$. The structure of the complex $[Mo(CO)(PEt_3)(\eta^3\text{-}anti\text{-}1\text{-}MeC_3H_4)(\eta^5\text{-}C_9H_7)]$ was established by single-crystal *X*-ray crystallography. Crystals are monoclinic, space group $P2_1/n$ with $a = 10.038(2)$, $b = 17.291(4)$, $c = 11.346(3)$ Å, $\beta = 95.000(18)°$, and $Z = 4$. Using 3 887 reflections measured on a four-circle diffractometer at room temperature, the structure has been refined to R 0.0344, R' 0.0459. The molecule adopts an *exo*-conformation with the methyl substituent of the allyl ligand in an *anti*-position *cis* to the carbonyl ligand. Treatment of the complex $[Mo\{P(OMe)_3\}_2(\eta\text{-}HC_2Bu^t)(\eta\text{-}C_5H_5)][BF_4]$ with $NaBH_4$ or $K[BHBu^s{}_3]$ in the presence of excess $P(OMe)_3$ gives the σ-vinyl complex $[Mo\{P(OMe)_3\}_3\{\sigma\text{-}(E)\text{-}CH{=}CHBu^t\}(\eta\text{-}C_5H_5)]$, structurally identified by n.m.r. spectroscopy and *X*-ray crystallography. Crystals are monoclinic, space group $P2_1/c$ with $a = 11.731(3)$, $b = 12.796(3)$, $c = 18.827(4)$ Å, $\beta = 92.33(2)°$, and $Z = 4$. Using 7 437 intensity data, measured at 195 K on a four-circle diffractometer, the structure has been refined to residuals $R = 0.026$, $R' = 0.026$. The molecule shows typical four-legged ' piano-stool ' geometry with the vinyl group adopting *E* stereochemistry, σ-bonded to the molybdenum atom. In contrast, the reaction of $K[BHBu^s{}_3]$ with $[Mo\{P(OMe)_3\}_2(\eta\text{-}HC_2Pr^i)(\eta\text{-}C_5H_5)][BF_4]$ in tetrahydrofuran at low temperature affords the allyl complex $[Mo\{P(OMe)_3\}_2(\eta^3\text{-}1,1\text{-}Me_2C_3H_3)(\eta\text{-}C_5H_5)]$. The n.m.r. spectra and mechanism of formation of these compounds are discussed.

The reaction of co-ordinated olefins with nucleophilic reagents has generated considerable interest [2] both academically and industrially; however, relatively little attention has been paid to the related reactions of nucleophiles with acetylenes co-ordinated to transition metals. Chisholm and Clark [3] showed that cationic Pt^{II} complexes of the type *trans*-$[Pt(Me)L_2(\eta\text{-}alkyne)][PF_6]$ (L = tertiary phosphine or arsine) react with methanol to form β-methoxyvinyl or methoxycarbene complexes, and more recently it has been reported [4,5] that the iron complex $[Fe(CO)(PPh_3)(\eta\text{-}MeC_2Me)(\eta\text{-}C_5H_5)][BF_4]$ reacts with a range of nucleophiles to form stable 18-electron σ-(*E*)-vinyl complexes. In contrast, we have noted [6] that the formally co-ordinatively unsaturated molybdenum cations $[Mo\{P(OMe)_3\}_2(\eta\text{-}MeC_2Me)A][BF_4]$ (A = $\eta\text{-}C_5H_5$ or $\eta^5\text{-}C_9H_7$) react with BH_4^- to form η^3-allyl complexes, and that the corresponding reaction of the 3,3-dimethylbut-1-yne complex affords a σ-vinyl species, which rearranges thermally to form an alkylidyne complex. In this paper we report a detailed investigation of the η^3-allyl complex-forming reaction, and the structural characterisation of key compounds.

Results and Discussion

Reaction of $[Mo\{P(OMe)_3\}_2(\eta\text{-}MeC_2Me)(\eta\text{-}C_5H_5)][BF_4]$ or $[Mo\{P(OMe)_3\}_2(\eta\text{-}MeC_2Me)(\eta^5\text{-}C_9H_7)][BF_4]$ [7,8] with $NaBH_4$ in tetrahydrofuran (thf) in the presence of $P(OMe)_3$ at room temperature affords the crystalline η^3-*anti*-1-methylallyl complexes (1) (yellow) and (2) (red). As an alternative to $NaBH_4$, ' potassium selectride ' † readily reacts with these cations to give identical products in comparable yields. As a result of the greater solubility of this reducing agent in thf, the reaction is rapid, even at −78 °C, and occurs without the need for the presence of free trimethyl phosphite. This reaction is quite general, the salts $[Mo\{P(OMe)_3\}_2(\eta\text{-}MeC_2R)(\eta\text{-}C_5H_5)][BF_4]$ (R = Et or Pr^i) and $[Mo(Ph_2PCH{=}CHPPh_2)(\eta\text{-}MeC_2Me)(\eta\text{-}C_5H_5)][BF_4]$ being reduced to the corresponding η^3-*anti*-1-substituted allyl complexes (3), (4), and (5), isolated as crystalline materials, and characterised by elemental analysis (Table 1), ^{13}C, ^{31}P (Table 2), and ^1H n.m.r. spectroscopy (Table 3).

In all cases the $^{13}C\text{-}\{^1H\}$ spectra show a singlet around 70 p.p.m. (±5 p.p.m.) ($SiMe_4$ reference) assignable to the central carbon atom of the η^3-allyl group. The terminal carbons of the allyl fragment resonate upfield of this signal and as a result of ^{31}P coupling occur as multiplets, being the X portion of an ABX system. The carbon bearing an alkyl substituent (Me, Et, or Pr^i) is downfield of the unsubstituted terminal carbon resonance, and the degree of deshielding of this signal is dependent on the electron-donating ability of the alkyl group, as would be expected. Though ^{13}C spectroscopy was

---

* Carbonyl(η^5-indenyl)(η^3-*anti*-1-methylallyl)(triethylphosphine)molybdenum(II) and [σ-(*E*)-2-t-butylvinyl](η-cyclopentadienyl)tris(trimethyl phosphite)molybdenum(II).

Supplementary data available (No. SUP 23528, 71 pp.): observed and calculated structure factors, thermal parameters, H-atom co-ordinates, full bond length and bond angle data for compound (8), least-squares planes and non-bonded contacts for compound (7). See Notices to Authors No. 7, *J. Chem. Soc., Dalton Trans.*, 1981, Index issue.

Non-S.I. unit employed: 1 cal = 4.184 J.

† Registered trade name (Aldrich); $K[BHBu^s{}_3]$.

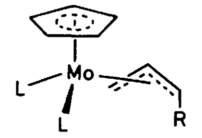

exo

[1a; R = Me, L = P(OMe)$_3$]
[3a; R = Et, L = P(OMe)$_3$]
[4a; R = Pr^i, L = P(OMe)$_3$]
[5a; R = Me, L$_2$ = Ph$_2$PCH=CHPPh$_2$]

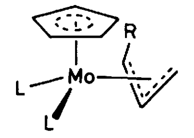

endo

(1b)
(3b)
(4b)
(5b)

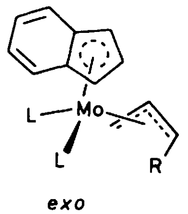

exo
(2a; R = Me)

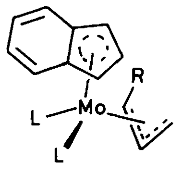

endo
(2b; R = Me)

used to confirm the existence of an η^3-allyl ligand the stereochemistry around that ligand was deduced by ^{1}H n.m.r. The signals associated with the allyl protons were broad and featureless, and without broad-band ^{31}P decoupling, assignments could be made only on the basis of chemical shift, but removing the ^{31}P–^{1}H couplings allowed the measurement of the major ^{1}H–^{1}H coupling constants. In all cases the central proton resonates at lowest field, and for the η-cyclopentadienyl systems this is around 3.7 p.p.m.

The proton on the substituted carbon occurs at 3.0 p.p.m. (±0.2 p.p.m.) and the protons on the unsubstituted carbon close together in the region of 2.1 p.p.m. (±0.2 p.p.m.). The splitting pattern of the central proton is characteristic overlapping doublet of triplets. The coupling constant associated with the doublet is larger by about 3 Hz than that responsible for the triplet, which is consistent with *one* J_{ca} and *two* J_{cs} couplings (see Table 3), indicating that the alkyl group is in the *anti*-position. This stereochemistry was confirmed by *X*-ray crystallography (see below).

The ^{1}H spectrum of (1) was temperature invariant; however, the corresponding spectrum (Table 3) and the ^{13}C-{^{1}H} and ^{31}P-{^{1}H} spectra of the η^5-indenyl complex (2) at −40 °C showed resonances corresponding to the presence of both *exo*- and *endo*-isomers, suggesting that whilst the η-cyclopentadienyl complex undergoes rapid *exo–endo* isomerisation the steric effect of the indenyl ligand raises the barrier to isomerisation sufficiently for the dynamic process to be frozen out. It is interesting that calculations [9] with the system [Mo(CO)$_2$(η-C$_3$H$_5$)(η-C$_5$H$_5$)] show there is a substantial (46 kcal mol^{-1}) barrier to a simple rotation about the Mo–allyl axis suggesting that alternative pathways for isomerisation may be involved.

The unsymmetrical cation [Mo(CO)(PEt$_3$)(η-MeC$_2$Me)(η-C$_5$H$_5$)][BF$_4$] reacts with both NaBH$_4$ and K[BHBu$^s_3$] in thf solvent to give after work-up a yellow solution showing four terminal carbonyl bands in its solution i.r. spectrum. The major product (6a) (70%; ν_{CO} 1 825 cm^{-1}) was separated from the three minor components (6b), (6c), and (6d) (ν_{CO} 1 843, 1 835, and 1 829 cm^{-1}), which were present in approximately equal proportions, by column chromatography, and characterised by elemental analysis (Table 1) and n.m.r. spectroscopy (Tables 2 and 3). Surprisingly, the analogous η^5-indenyl cation afforded only one isomeric product (7), which had identical ^{1}H and ^{13}C n.m.r. spectra except for the large upfield shift of the central proton on the η^3-allyl ligand relative to the major isomer (6a) from the η-cyclopentadienyl system. This large shift [10] (>4 p.p.m.) is a consequence of the orientation of the allyl fragment in the *exo*-configuration, and the magnetic anisotropy associated with the six-membered ring of the η^5-indenyl ligand. That (6a) and (7) have the same stereochemistry is further demonstrated by the fact that each exhibits the same degree of phosphorus coupling to the *anti*-proton (Table 3), all the other protons showing very small ^{31}P coupling. Charrier and co-workers,[11] while investigating the related complexes [Mo(CO){P(OMe)$_3$}(*exo*-η^3-2-RXCO–C$_3$H$_4$)(η-C$_5$H$_5$)] (*e.g.* R = Me, X = O or S) observed that ^{31}P–^{1}H coupling was greatest to the *anti*-proton *cis* to the phosphite. The order of this coupling (11 Hz) is identical to that observed (Table 3) with (6a) and (7) suggesting the illustrated structures for these complexes, in which the *anti*-methyl substituent is *trans* to the PEt$_3$ ligand.

In order to provide a firm basis for a discussion of the mechanism of formation of these η^3-allyl complexes it was thought necessary to confirm the stereochemistry of these molecules, and therefore a single-crystal *X*-ray diffraction study was carried out with the unsymmetrical complex (7). The complex crystallises as discrete molecules with no severe intermolecular contacts. A perspective view of a single molecule, together with the atomic numbering scheme adopted is given in Figure 1. Hydrogen atoms of the indenyl ligand are not labelled, but carry the same number of the carbon to

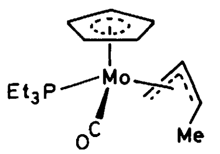

(6a)

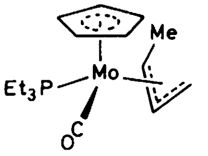

(6b)

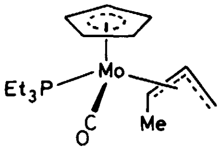

(6c)

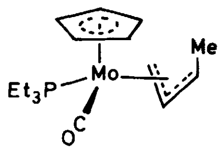

(6d)

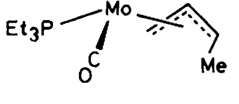

(7)

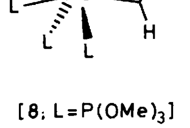

[8; L = P(OMe)$_3$]

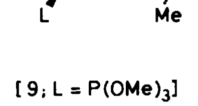

[9; L = P(OMe)$_3$]

Table 1. Analytical,[a] mass spectroscopic,[a,b] and i.r.[c] data for the complexes $[MoLL^1(\eta^3\text{-allyl})A]$ ($A = \eta\text{-}C_5H_5$ or $\eta^5\text{-}C_9H_7$)

Complex	Colour	Yield (%)	ν_{CO}/cm^{-1}	Analysis C (%)	Analysis H (%)	Analysis *M*
(1) $[Mo\{P(OMe)_3\}_2(\eta^3\text{-}anti\text{-}1\text{-}MeC_3H_4)(\eta\text{-}C_5H_5)]$	Yellow	65	—	38.5 (38.8)	6.7 (6.5)	466 (466)
(2) $[Mo\{P(OMe)_3\}_2(\eta^3\text{-}anti\text{-}1\text{-}MeC_3H_4)(\eta^5\text{-}C_9H_7)]$	Red	70	—	49.9 (44.4)	6.6 (6.2)	516 (516)
(3) $[Mo\{P(OMe)_3\}_2(\eta^3\text{-}anti\text{-}1\text{-}EtC_3H_4)(\eta\text{-}C_5H_5)]$	Yellow	73	—	40.5 (40.2)	6.7 (7.0)	480 (480)
(4) $[Mo\{P(OMe)_3\}_2(\eta^3\text{-}anti\text{-}1\text{-}Pr^iC_3H_4)(\eta\text{-}C_5H_5)]$	Yellow	81	—	41.9 (41.5)	7.4 (7.0)	494 (494)
(5) $[Mo\{Ph_2PCH\}_2(\eta^3\text{-}anti\text{-}1\text{-}MeC_3H_4)(\eta\text{-}C_5H_5)]$	Red	65	—	67.1 (68.6)	5.8 (5.6)	614 (614)
(6a) $[Mo(CO)(PEt_3)(\eta^3\text{-}anti\text{-}1\text{-}MeC_3H_4)(\eta\text{-}C_5H_5)]$	Yellow	70	1 825	53.0 (53.0)	7.5 (7.5)	364 (364)
(7) $[Mo(CO)(PEt_3)(\eta^3\text{-}anti\text{-}1\text{-}MeC_3H_4)(\eta^5\text{-}C_9H_7)]$	Red	70	1 826	59.0 (58.3)	7.6 (7.1)	414 (414)
(9) $[Mo\{P(OMe)_3\}_2(\eta^3\text{-}1,1\text{-}Me_2C_3H_3)(\eta\text{-}C_5H_5)]$	Yellow	68	—	40.5 (40.2)	6.6 (6.7)	480 (480)

[a] Calculated values are given in parentheses. [b] Parent ion ^{98}Mo. [c] Measured in hexane.

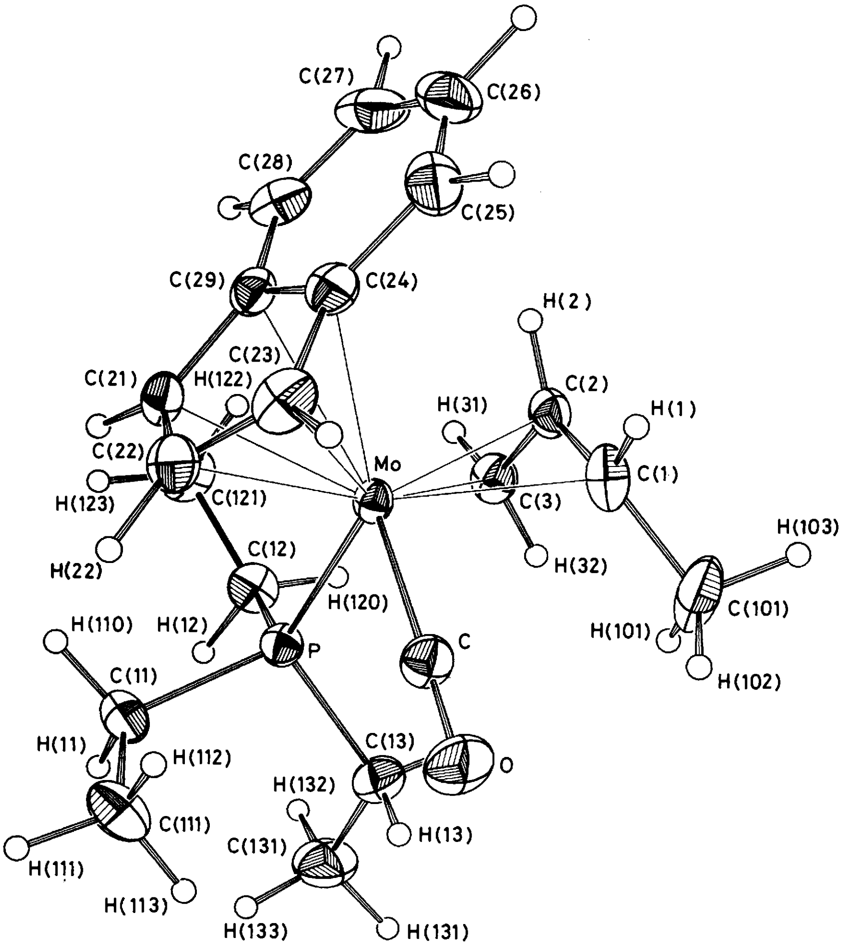

Figure 1. Molecular structure of $[Mo(CO)(PEt_3)(\eta^3\text{-}anti\text{-}1\text{-}MeC_3H_4)(\eta^5\text{-}C_9H_7)]$ (7). For non-hydrogen atoms, thermal ellipsoids are drawn at the 50% probability level. Hydrogen atoms have an artificial radius of 0.1 Å for clarity; H(121) is obscured by C(121) and H(130) by O

which they are bound. Table 4 lists the internuclear distances and Table 5 important interbond angles. Fractional atomic co-ordinates are in Table 6.

This study represents an addition to the small but growing number[12] of structural studies of species of the general type $[MLL^1X(\text{allyl})]$, where M = Mo or W, L and L^1 are neutral two-electron donor ligands, and X = cyclopentadienyl or a derivative; compound (7) represents the first structurally studied indenyl derivative. Hoffmann and co-workers[9] found (EHMO calculations) that for the reference molecule $[Mo(CO)_2(\eta\text{-}C_3H_5)(\eta\text{-}C_5H_5)]$, the *endo*-geometry is slightly favoured. We believe that the *exo*-stereochemistry displayed in the crystal of (7) represents the minimum energy conformation for this molecule, and results from the minimisation of intramolecular contacts. In (7) the disposition of the six-membered ring of the indenyl ligand with respect to the $Mo(CO)(PEt_3)$ fragment is clearly sterically preferred since we find two non-bonded contacts, H(22) ··· H(12) 2.26 and H(21) ··· H(110) 2.34 Å, just below twice the van der Waals radius for hydrogen. Given this orientation it is apparent that

Table 2. Carbon-13 n.m.r. data for the complexes [MoLL^1(η^3-allyl)A] (A = η-C_5H_5 or η^5-C_9H_7)]

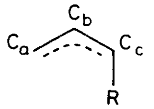

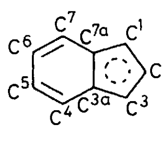

Complex	L	L^1	η^3-allyl	δ/p.p.m.[a]
(1) [b,c]	P(OMe)$_3$	P(OMe)$_3$	1-MeC$_3$H$_4$	86 (s, C_5H_5), 73.8 (s, C_b), 50.6 (m, PO*C*H$_3$), 47.3 [dd, C_c, J(CP) + J(CP′) 11.7], 30.1 [dd, C_a, $\lvert J(\mathrm{CP}) + J(\mathrm{CP'})\rvert$ 10.7], 20.2 (s, Me)
(2a)/(2b) [d,e]	P(OMe)$_3$	P(OMe)$_3$	1-MeC$_3$H$_4$	126.8, 126.8, 124.9, 124.6, 124.1, 123.8, 123.2, 122.0 (C^4, C^5, C^6, C^7, *exo* and *endo*), 111.8 [d, $\lvert J(\mathrm{CP}) + J(\mathrm{CP'})\rvert$ 4.9], 110.4 [d, $\lvert J(\mathrm{CP}) + J(\mathrm{CP'})\rvert$ 4.9], 108.4 [t, $\lvert J(\mathrm{CP}) + J(\mathrm{CP})\rvert$ 5.0], 105.4 [t, $\lvert J(\mathrm{CP}) + J(\mathrm{CP'})\rvert$ 5.0], (C^{3a}, C^{7a}, *exo* and *endo*), 85, 82.3, 80.2, 80.2, 78.7, 77.9, 74.2, 73.9, (C^1, C^2, C^3, C^6, *exo* and *endo*), 51.7 [dd, $\lvert J(\mathrm{CP}) + J(\mathrm{CP'})\rvert$ 15.6], 51 [dd, $\lvert {}^2J(\mathrm{CP}) + {}^4J(\mathrm{CP})\rvert$ 7.8], [PO*C*H$_3$, *exo* and *endo*], 55.4 [dd, $\lvert J(\mathrm{CP}) + J(\mathrm{CP'})\rvert$, 21.5], 48.8 [dd, $\lvert J(\mathrm{CP}) + J(\mathrm{CP'})\rvert$ 11.7], 46.0 (C_c, *exo* and *endo*), 44.1 [d, $\lvert J(\mathrm{CP}) + J(\mathrm{CP'})\rvert$ 6.8], 39.2 [dd, $\lvert J(\mathrm{CP}) + J(\mathrm{CP'})\rvert$ 19.5], 30.0 [C_a, *exo* and *endo*], 16.9 [d, $\lvert J(\mathrm{CP}) + J(\mathrm{CP'})\rvert$ 3.9], 16.2 (s) (Me, *exo* and *endo*)
(3) [b,f]	P(OMe)$_3$	P(OMe)$_3$	1-EtC$_3$H$_4$	85.8 (s, C_5H_5), 72.5 (s, C_b), 56.7 [d, C_c, $\lvert J(\mathrm{CP}) + J(\mathrm{CP'})\rvert$ 9.8], 50.6 [dd, PO*C*H$_3$, $\lvert J(\mathrm{CP}) + J(\mathrm{CP'})\rvert$ 13.7], 29.9 [d, C_a, $\lvert J(\mathrm{CP}) + J(\mathrm{CP'})\rvert$ 9.8], 29.4 (s, *C*H$_2$CH$_3$), 22.2 (s, CH$_2$*C*H$_3$)
(4) [b,g]	P(OMe)$_3$	P(OMe)$_3$	1-Pr^{i}C$_3$H$_4$	85.1 (s, C_5H_5), 72.1 (s, C_b), 63.6 [t, C_c, $\lvert J(\mathrm{CP}) + J(\mathrm{CP'})\rvert$ 10.7], 50.7 [d, PO*C*H$_3$, J(CP) 2.9], 34.9 (s, *C*HMeMe′), 31.8 (s, CH*Me*Me′), 30.3 [t, C(a), $\lvert J(\mathrm{CP}) + J(\mathrm{CP'})\rvert$ 10.7 Hz], 24.4 (s, CHMe*Me′*)
(5) [b,h]	Ph$_2$PCH=CHPPh$_2$		1-MeC$_3$H$_4$	152.4 [t, Ph$_2$P*C*H=, $\lvert J(\mathrm{CP}) + J(\mathrm{CP'})\rvert$ 67.4], 152.1 [t, Ph$_2$P*C*H=, $\lvert J(\mathrm{CP}) + J(\mathrm{CP'})\rvert$ 68.4], 142.3 (dd, Ph$_2$P), 140.8 (dd, Ph$_2$P), 136.9 (d, Ph$_2$P), 135.9 (d, Ph$_2$P), 132.5 (d, Ph$_2$P), 132.2 (d, Ph$_2$P), 131.8 (d, Ph$_2$P), 131.5 (d, Ph$_2$P), 128.5 (s), 128.3 (s), 128.1 (s), 127.9 (s), 127.8 (s) [aromatic carbons], 88 (s, C_5H_5), 68.3 (s, C_b), 46.2 [d, C_c, $\lvert J(\mathrm{CP}) + J(\mathrm{CP'})\rvert$ 4.9], 30.0 [d, C_a, $\lvert J(\mathrm{CP}) + J(\mathrm{CP'})\rvert$ 4.9], 20.7 [t, Me, $\lvert J(\mathrm{CP}) + J(\mathrm{CP'})\rvert$ 3.8]
(6a) [b]	PEt$_3$	CO	1-MeC$_3$H$_4$	89.4 (s, C_5H_5), 64.9 (s, C_b), 48.8 (s, C_c), 33.2 [d, C_a, J(CP) 13.7], 23.0 [d, PC*H*$_2$CH$_3$, J(CP) 25.9], 15.2 (s, Me), 8.3 (s, PCH$_2$*C*H$_3$)
(7) [b]	PEt$_3$	CO	1-MeC$_3$H$_4$	124.6 (s), 123.8 (s), 122.8 (s), 121.6 (s), 110.9 (s), 108.8 (s), 87.1 (s), 81.6 (s), 81.2 (s) (η^5-indenyl), 77.4 (s, C_b), 60.3 (s, C_c), 40.9 [d, C_a, J(CP) 13.7], 22.8 [d, P*C*H$_2$CH$_3$, J(CP) 25.9], 16.2 (s, Me), 8.4 (s, PCH$_2$*C*H$_3$)
(9) [b,i]	P(OMe)$_3$	P(OMe)$_3$	1,1-Me$_2$C$_3$H$_3$	87.6 (s, C_5H_5), 67.4 (s, C_b), 63.2 [dd, C_c, $\lvert J(\mathrm{CP}) + J(\mathrm{CP'})\rvert$ 15.6], 51.6 [dd, POC*H*$_3$, $\lvert J(\mathrm{CP}) + J(\mathrm{CP'})\rvert$ 14.1], 51.3 [dd, POC*H*$_3$, $\lvert J(\mathrm{CP}) + J(\mathrm{CP'})\rvert$ 14.1], 31.4 (s, *syn*-Me), 25.6 [dd, C_a, $\lvert J(\mathrm{CP}) + J(\mathrm{CP'})\rvert$ 18.0], 25.0 [d, *anti*-Me, $\lvert J(\mathrm{CP}) + J(\mathrm{CP'})\rvert$3.9]

[a] Downfield from SiMe$_4$; J values in Hz. [b] In C$_6$D$_6$ at 303 K. [c] ^{31}P-{^{1}H} resonances (C$_6$D$_6$, 303 K): δ_A 208.2, δ_B 205.9, J(AB) 87.9 Hz. [d] In C$_6$D$_6$CD$_3$ at 233 K. [e] ^{31}P-{^{1}H} resonances (C$_6$D$_6$CD$_3$, 233 K): δ_A 210.1, δ_B 205.6, J(AB) 90.3 Hz; δ_A 204.2, δ_B 202.6, J(AB) 107.4 Hz (*exo* and *endo* isomers). [f] ^{31}P-{^{1}H} resonances (C$_6$D$_6$, 303 K): δ_A 208.2, δ_B 205.8, J(AB) 87.9 Hz. [g] ^{31}P-{^{1}H} resonances (C$_6$D$_6$, 303 K): 205 (s). [h] ^{31}P-{^{1}H} resonances (C$_6$D$_6$, 303 K): δ_A 106.1, δ_B 105.1, J(AB) 7.3 Hz. [i] ^{31}P-{^{1}H} resonances (C$_6$D$_6$, 303 K): δ_A 201.6, δ_B 199.9, J(AB) 110.1 Hz.

either a *syn*- or *anti*-C$_3$H$_4$Me ligand of an *endo*-(7) would suffer severe steric congestion with the atoms CH(25)–CH(29).

The indenyl function is clearly η^5-bonded to molybdenum, but displays the asymmetric co-ordination commonly observed [13] with this ligand. Thus the Mo–C(21), Mo–C(22), and Mo–C(23) bond lengths [2.335(3)—2.359(3) Å] are considerably shorter than the links between metal and bridging carbon atoms: Mo–C(24) 2.436(3) and Mo–C(29) 2.458(3) Å. Similar asymmetry sometimes occurs in analogous η-C$_5$H$_5$ complexes [12] and, in both classes of compound, may be described as a slipping of the metal atom across the η-bonded face, *i.e.* the ligand co-ordination changes from η^5 to η^3. In the case of the indenyl species, however, the limit of such a distortion has a particular significance since the free double bond ultimately generated [C(24)–C(29) in compound (7)] may be stabilised as part of an aromatic system. Indeed, η^5 to η^3 slippage has been invoked [14] as a primary reason for the substantially enhanced reactivity towards ligand substitution of indenyl rhodium(I) complexes over their η-C$_5$H$_5$ analogues. The slipping distortion may be quantified in terms of either an angular [12b,13c] slip, ψ, or a translational [13c] slip, Δ. For compound (7), $\psi = 3.7°$ and $\Delta = 0.133$ Å.

A corollary to the above asymmetric η^5-bonding and the partial concentration of π-electron density in C(24)–C(29) that accompanies it is a distinct localisation in the six-membered ring at C(25)–C(26) and C(27)–C(28) [1.341(6) and 1.363(6) Å]; both these bonds are significantly * shorter than C(24)–C(25), C(26)–C(27), and C(28)–C(29) [1.422(5), 1.408(7), and 1.416(5) Å respectively]. Similar bond localisation is apparent in other precise structural studies [13a,13b,13e] of co-ordinated indenyl ligands. Both the five- and six-membered rings of the indenyl fragment are planar within experimental error (in SUP 23528) and closely coplanar (dihedral angle 2.0°).

---

* The smallest difference is between C(27)–C(28) (x_i) and C(26)–C(27) (x_j), and is 0.045(9) Å, where the estimated standard deviation is given by $(\sigma_i^2 + \sigma_j^2)^{\frac{1}{2}}$; hence $|x_i - x_j| = 5.06$.

Table 3. Hydrogen-1 n.m.r. data for the complexes [MoLL^1(η^3-allyl)A] (A = η-C$_5$H$_5$ or η^5-C$_9$H$_7$)

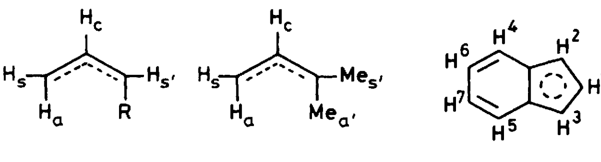

Complex	L	L^1	η^3-allyl	δ/p.p.m.^{a}
(1) ^{b,c}	P(OMe)$_3$	P(OMe)$_3$	1-MeC$_3$H$_4$	4.58 (s, 5 H, C$_5$H$_5$), 3.73 (dt, 1 H, C$_c$, J_{ca} 9.5, $J_{cs} = J_{cs'} = 6.0$), 3.37 (s, br, 18 H, PO*Me*), 3.14 (quintet, 1 H, H$_{s'}$, $J_{s'c} = J_{s'a'} = 6.0$), 2.28 (d, 1 H, H$_s$, J_{sc} 6.5), 2.25 (d, 1 H, H$_a$, J_{ac} 9.0), 1.31 (d, 3 H, Me$_{a'}$, $J_{a's'}$ 6.3)
(2a)/(2b) ^{d}	P(OMe)$_3$	P(OMe)$_3$	1-MeC$_3$H$_4$	7.2—6.4 [m, 4 H, H(4)—H(7)], 5.80, 5.54 [s, br, 1 H, H(1) or H(3)], 5.40, 5.23 [t, 1 H, H(2), J(HH) 1.5], 5.09, 5.04 [s, br, 1 H, H(3) or H(1)], 3.37 (m, 18 H, PO*CH$_3$*), 3.70 (*endo*), −1.34 (*exo*) [dt, 1 H, H$_c$, J_{ca} 10, $J_{cs} = J_{cs'} = 7$], 2.84 (*endo*) 2.64 (*exo*), [m, 1 H, H$_{s'}$], 1.51 (*endo*), 1.10 (*exo*), [d, 1 H, H$_s$, J_{cs} 7.5], 1.10 (*endo*), 1.71 (*exo*), [d, 1 H, H$_a$, J_{ca} 10.0], 0.47 (*endo*), 1.03 (*exo*), [d, 3 H, Me, $J_{s'\mathrm{Me}}$ 6.2]
(3) ^{b,c}	P(OMe)$_3$	P(OMe)$_3$	1-EtC$_3$H$_4$	4.64 (s, 5 H, C$_5$H$_5$), 3.69 [dt, 1 H, H$_c$, J_{ca} 9.8, $J_{cs} = J_{cs'} = 6.9$], 3.40 (s, 9 H, PO*Me*), 3.36 (s, 9 H, PO*Me*), 3.04 (quartet, 1 H, H$_{s'}$, J 6), 2.32 [dd, 1 H, H$_s$, J_{sc} 6.4, $J_{ss'}$ 1.4], 2.26 [d, 1 H, H$_a$, J_{ac} 9.6], 1.48 [m, 1 H, C*H*(H′)Me], 1.18 [t, 3 H, CH(H′)*Me*, J 6.8], 0.88 [m, 1 H, CH(*H′*)Me]
(4) ^{b,c}	P(OMe)$_3$	P(OMe)$_3$	1-Pr^{i}C$_3$H$_4$	4.70 (s, 5 H, C$_5$H$_5$), 3.68 [dt, 1 H, H$_c$, J_{ca} 9.3, $J_{cs} = J_{cs'} = 6.5$], 3.49 (s, 9 H, PO*Me*), 3.37 (s, 9 H, PO*Me*), 2.85 [t, 1 H, H$_{s'}$, J 6.8], 2.16 [dd, 1 H, H$_s$, J_{sc} 6.7, J_{ss}, 2.1 Hz], 2.08 [d, 1 H, H$_a$, J_{ac} 9.1], 1.30 [s, br, 3 H, CH*Me*Me′], 1.02 [s, br, 3 H, CHMe*Me′*]
(5) ^{b,c}	Ph$_2$PCH=CHPPh$_2$		1-MeC$_3$H$_4$	7.8—7.0 (m, 22 H, aromatic and olefinic), 4.06 (s, br, 5 H, C$_5$H$_5$), 2.70 (m, 2 H, H$_c$ and H$_{s'}$), 2.14 [d, 1 H, H$_a$, J_{ac} 9], 1.90 [d, 1 H, H$_s$, J_{sc} 6.0], 1.38 [d, 3 H, Me, $J_{s'\mathrm{Me}}$ 6.0]
(6) ^{b,c}	PEt$_3$	CO	1-MeC$_3$H$_4$	4.60 (s, 5 H, C$_5$H$_5$), 3.74 [dt, 1 H, H$_c$, J_{ca} 12.9, $J_{cs} = J_{cs'} = 7.1$], 3.34 [quintet, 1 H, H$_{s'}$, J 6.7], 2.20 [ddd, 1 H, J_{sc} 7.0, J(H$_s$)P 3.5, J_{ss}, 1.9] 0.46—1.1 (m, 6 H, P*CH$_2$*CH$_3$), 1.35 [d, 3 H, Me$_{a'}$, $J_{s'a'}$ 6.2], 1.0—0.7 (m, 9 H, PCH$_2$*CH$_3$*), 0.46 [t, 1 H, H$_a$, J(H$_a$)P 12.2, J_{ac} 12.5]
(7) ^{b,c}	PEt$_3$	CO	1-MeC$_3$H$_4$	6.9—6.5 [m, 4 H, H(4)—H(7)], 5.72 [t, 1 H, H(1), J(HH) 1.5], 5.08 [m, 2 H, H(2) and H(3)], 3.09 [quintet, 1 H, H$_{s'}$, J(HH) 6.7], 1.76 [ddd, 1 H, H$_s$, $J_{ss'}$ 2.8, J_{sc} 8.5, J(H$_s$P) 5.7], 1.8—1.1 (m, 6 H, P*CH$_2$*CH$_3$), 1.28 [d, 3 H, Me$_{a'}$, $J_{s'a'}$ 6.0], 1.0—0.7 (m, 9 H, PCH$_2$*CH$_3$*), 0.54 [dd, 1 H, H$_a$ J(H$_a$P) 11.0], −1.48 [dt, 1 H, H$_c$, J_{ca} 11.6, $J_{cs'} = J_{cs} = 8.1$]
(9)	P(OMe)$_3$	P(OMe)$_3$	1,1-Me$_2$C$_3$H$_3$	4.76 (s, 5 H, C$_5$H$_5$), 3.76 [dd, 1 H, H$_c$, J_{ca} 8.6, J_{cs} 6.8], 3.46 [d, 18 H, PO*Me*, $\lvert J(\mathrm{HP}) + J(\mathrm{HP'})\rvert$ 9.7], 2.08 [m, 1 H, H$_s$, J_{sc} 7.0, $\lvert J(\mathrm{HP}) + J(\mathrm{HP'})\rvert$ 2.0], 1.91 (s, 3 H, Me$_{s'}$), 1.50 [m, 1 H, H$_a$, J_{ac} 9.3, $\lvert J(\mathrm{HP}) + J(\mathrm{HP'})\rvert$ 11.9], 1.23 (s, 3 H, Me$_{a'}$)

^{a} Downfield from SiMe$_4$; J values in Hz. ^{b} Measured at 303 K unless otherwise stated. ^{c} In C$_6$D$_6$. ^{d} In C$_6$D$_6$CD$_3$ at 233 K.

Table 4. Bond distances (Å) for [Mo(CO)(PEt$_3$)(η^3-*anti*-1-MeC$_3$H$_4$)(η^5-C$_9$H$_7$)] (7) [*]

Mo–P	2.427 4(8)	Mo–C(29)	2.458(3)	C(21)–C(22)	1.401(5)	C(24)–C(29)	1.434(4)
Mo–C	1.892(3)	C–O	1.177(4)	C(22)–C(23)	1.416(6)	C(1)–C(2)	1.396(5)
Mo–C(1)	2.365(3)	P–C(11)	1.854(3)	C(23)–C(24)	1.425(5)	C(2)–C(3)	1.410(5)
Mo–C(2)	2.197(3)	P–C(12)	1.840(3)	C(24)–C(25)	1.422(5)	C(1)–C(101)	1.502(6)
Mo–C(3)	2.323(3)	P–C(13)	1.848(3)	C(25)–C(26)	1.341(6)	C(1)–H(1)	0.88(5)
Mo–C(21)	2.359(3)	C(11)–C(111)	1.527(5)	C(26)–C(27)	1.408(7)	C(2)–H(2)	0.99(4)
Mo–C(22)	2.335(3)	C(12)–C(121)	1.519(5)	C(27)–C(28)	1.363(6)	C(3)–H(31)	0.90(4)
Mo–C(23)	2.338(3)	C(13)–C(131)	1.529(6)	C(28)–C(29)	1.416(5)	C(3)–H(32)	0.99(5)
Mo–C(24)	2.436(3)			C(29)–C(21)	1.427(4)		

[*] Estimated standard deviations are given in parentheses in Tables 4—9.

At an angle of *ca.* 36° to the overall indenyl plane lies the plane of the allyl ligand. The Mo–C(2) bond length [C(2) is the inner allyl carbon atom] is 2.197(3) Å, substantially less than Mo–C(1) [2.365(3) Å] and Mo–C(3) [2.323(5) Å], C(1) and C(3) being the outer allyl carbons. In allyl complexes generally,[15] and with some exceptions [*] in *endo*-[MLL^1(allyl)(η-C$_5$H$_5$)] complexes specifically,[12b,12e] either the same pattern is observed or else no significant difference in M–C lengths is found.[16]

In (7) the methyl group C(101)H$_3$ is *cis* to CO, and adopts an *anti*-conformation. Within the Mo(C$_3$H$_4$Me) fragment the Mo–C(outer) bond lengths are significantly different with C(1) the further away by 0.042(4) Å, and, consistent with a similar effect, C(1)–C(2) is slightly shorter than C(2)–C(3). Both features may be rationalised in terms of the avoidance of

---

[*] The exceptions are [Mo(CO)$_2$(4-MeC$_6$H$_4$CH$_2$)(σ-C$_5$H$_5$)] in which the molybdenum atom is significantly closer to the exocyclic end of the allyl function,[12a] and [Mo(2,6-Me$_2$C$_6$H$_3$NC)$_2${(2,6-Me$_2$C$_6$H$_3$)-N=C$\overset{\cdots}{=}$C(CH$_2$Bu^t)$\overset{\cdots}{=}$C=N(2,6-Me$_2$C$_6$H$_3$)}(η-C$_5$H$_5$)] in which Mo–C (inner) exceeds Mo–C (outer) by *ca.* 0.13 Å as the result of intramolecular steric congestion.[12e]

Table 5. Important bond angles (°) for $[Mo(CO)(PEt_3)(\eta^3\text{-}anti\text{-}1\text{-}MeC_3H_4)(\eta^5\text{-}C_9H_7)]$ (7)

P-Mo-C	82.67(9)	C(2)-Mo-C(29)	92.45(11)	C-Mo-C(23)	92.81(13)	C(11)-P-C(12)	101.2(2)
P-Mo-C(1)	123.08(10)	C(3)-Mo-C(21)	118.68(12)	C-Mo-C(24)	122.12(13)	C(11)-P-C(13)	102.7(2)
P-Mo-C(2)	111.72(9)	C(3)-Mo-C(22)	153.40(12)	C-Mo-C(29)	149.72(12)	C(12)-P-C(13)	100.2(2)
P-Mo-C(3)	75.94(8)	C(3)-Mo-C(23)	147.83(12)	C(1)-Mo-C(2)	35.38(12)	P-C(11)-C(111)	114.7(3)
P-Mo-C(21)	86.90(8)	C(3)-Mo-C(24)	114.05(11)	C(1)-Mo-C(21)	146.62(12)	P-C(12)-C(121)	115.5(2)
P-Mo-C(22)	97.42(10)	C(3)-Mo-C(29)	100.94(11)	C(1)-Mo-C(22)	136.23(14)	P-C(13)-C(131)	117.0(3)
P-Mo-C(23)	132.01(9)	C(21)-Mo-C(22)	34.72(12)	C(1)-Mo-C(23)	101.40(13)	Mo-C-O	176.2(3)
P-Mo-C(24)	143.83(8)	C(21)-Mo-C(29)	34.39(10)	C(1)-Mo-C(24)	90.51(12)	C(1)-C(2)-C(3)	121.5(3)
P-Mo-C(29)	111.80(7)	C(22)-Mo-C(23)	35.28(13)	C(1)-Mo-C(29)	113.19(11)	C(2)-C(1)-C(101)	123.5(4)
C-Mo-C(1)	75.64(13)	C(23)-Mo-C(24)	34.65(12)	C(2)-Mo-C(3)	36.21(11)	C(29)-C(21)-C(22)	108.3(3)
C-Mo-C(2)	107.09(13)	C(24)-Mo-C(29)	34.08(11)	C(2)-Mo-C(21)	124.70(12)	C(21)-C(22)-C(23)	108.9(3)
C-Mo-C(3)	108.51(14)	Mo-P-C(11)	115.63(13)	C(2)-Mo-C(22)	144.59(13)	C(22)-C(23)-C(24)	107.7(3)
C-Mo-C(21)	127.24(13)	Mo-P-C(12)	119.49(10)	C(2)-Mo-C(23)	115.20(12)	C(23)-C(24)-C(29)	107.7(3)
C-Mo-C(22)	95.87(13)	Mo-P-C(13)	114.93(13)	C(2)-Mo-C(24)	87.33(12)	C(24)-C(29)-C(21)	107.3(3)

Table 6. Fractional atomic co-ordinates for $[Mo(CO)(PEt_3)(\eta^3\text{-}anti\text{-}1\text{-}MeC_3H_4)(\eta^5\text{-}C_9H_7)]$ (7)

Atom	*x*	*y*	*z*	Atom	*x*	*y*	*z*
Mo	0.504 02(2)	0.340 11(1)	0.695 24(2)	C(21)	0.442 0(3)	0.264 5(2)	0.526 3(3)
P	0.266 81(8)	0.353 52(4)	0.717 45(7)	C(22)	0.489 0(4)	0.335 9(2)	0.488 8(3)
C	0.500 6(3)	0.449 2(2)	0.707 0(3)	C(23)	0.626 0(4)	0.342 1(2)	0.529 0(3)
O	0.501 7(3)	0.517 3(1)	0.708 4(3)	C(24)	0.667 0(3)	0.272 5(2)	0.585 9(3)
C(1)	0.671 9(4)	0.369 3(2)	0.848 2(3)	C(25)	0.792 3(4)	0.244 2(3)	0.636 0(3)
C(2)	0.613 6(3)	0.296 5(2)	0.857 8(3)	C(26)	0.800 6(5)	0.172 9(3)	0.682 5(4)
C(3)	0.478 6(3)	0.288 2(2)	0.880 7(3)	C(27)	0.687 1(5)	0.125 3(3)	0.684 6(4)
C(101)	0.654 0(6)	0.434 4(2)	0.933 0(4)	C(28)	0.564 5(4)	0.149 0(2)	0.637 0(3)
C(11)	0.161 6(4)	0.382 1(2)	0.582 0(3)	C(29)	0.552 2(3)	0.223 0(2)	0.583 7(2)
C(12)	0.172 6(3)	0.270 4(2)	0.767 9(3)	H(1)	0.754(5)	0.369(3)	0.825(4)
C(13)	0.224 2(4)	0.427 3(2)	0.825 9(3)	H(2)	0.657(4)	0.249(2)	0.831(4)
C(111)	0.193 2(5)	0.461 7(3)	0.533 3(4)	H(31)	0.447(4)	0.239(3)	0.875(4)
C(121)	0.193 4(4)	0.194 6(2)	0.704 2(4)	H(32)	0.446(5)	0.328(3)	0.935(4)
C(131)	0.075 7(5)	0.440 6(3)	0.839 1(4)				

severe intramolecular crowding, in the former case between $C(101)H_3$ and the PEt_3 ligand, and in the latter case between $C(101)H_3$ and CH(25) and CH(26).

All substituents in the C(1)C(2)C(3) sequence lie out of the plane. Elevation angles (positive denoting bending towards the molybdenum atom) are at +12.3° for H(2), +6.4° and +7.7° for the *syn* hydrogens H(1) and H(31) respectively, and −36.3° and −32.0° for the *anti*-atoms C(101) and H(32). These figures are consistent with an inward rehybridisation of the allyl π molecular orbital on bonding to the metal. The H(31)− and H(32)−C(3)−Mo angles, for example, are identical at 111(3)°. The C(1)C(2)C(3) plane makes a dihedral angle of 6.3° to the Mo−C−P plane due entirely * to repulsion of the phosphine away from C(3) through intramolecular contact [H(32) · · · H(130) 2.26 Å, H(31) · · · H(120) and H(31) · · · H(122) just greater than the van der Waals sum at 2.48 and 2.45 Å respectively].

Molecular parameters within the MoCO and $MoPEt_3$ units are unexceptional. Mo−C is a little shorter, and C−O a little longer than the corresponding distances in the most comparable molecule, $[Mo(CO)_2(CH_2\overset{\cdots}{-}CH\overset{\cdots}{-}CH_2)(\eta\text{-}C_5H_5)]$.[12d] There is only one intermolecular contact (2.22 Å) between H(25) and H(12) of an adjacent unit cell (1 + *x*, *y*, *z*). A crystal packing diagram, viewed nearly along the *a* axis, is given in Figure 2.

The formation of the η^3-allylic complexes (1)—(7) clearly involves a hydrogen migration reaction, and it is interesting that reaction of $[Mo\{P(OMe)_3\}_2(\eta\text{-}MeC_2Me)(\eta\text{-}C_5H_5)][BF_4]$ with $NaBD_4$ in thf leads to the exclusive formation of the complex $[Mo\{P(OMe)_3\}_2(\eta^3\text{-}anti\text{-}CH_2\overset{\cdots}{-}CH\overset{\cdots}{-}CDMe)(\eta\text{-}C_5H_5)]$. A reaction pathway, which explains this observation, and also the formation of the compounds (1)—(7), is illustrated in Scheme 1, where an 18-electron molybdenum cation, in which the acetylene functions as a four-electron donor,[8,17] reacts with a source of H^-, the anions BH_4^- or $BHBu^s{}_3{}^-$. It is assumed [8] that on approach of the hydride source the acetylene ' switches ' its bonding mode to that of a two-electron donor so as to accommodate the incoming anion. The (2e) η^2-bonded acetylene present in the resultant hydrido(acetylene) complex is free to rotate, thus allowing it to achieve the orientation required for a *cis*-coplanar migration of the hydrogen from the metal onto carbon resulting in the formation of a (1e) σ-bonded vinyl complex, in which the molybdenum is co-ordinatively unsaturated (16 electron).

The resultant vinyl complex can undergo a β-hydrogen elimination reaction to regenerate the hydrido(acetylene) complex or alternatively rotation can occur about the $Mo-C_\alpha$ bond so as to allow access to a conformational isomer, in which a β-hydrogen of a methyl group is positioned to interact with the molybdenum centre. Such an interaction would be expected to lead to a β-hydrogen elimination with the formation of a hydrido(allene) complex, there being precedent for such a reaction in the observation [18] that the iridium(I) complex $[Ir\{\sigma\text{-}(E)\text{-}CMe{=}CH(Me)\}(CO)(PPh_3)_2]$ on heating (90 °C) isomerises to form $[Ir(\eta^3\text{-}syn\text{-}CH_2\overset{\cdots}{-}CH\overset{\cdots}{-}CHMe)(CO)(PPh_3)_2]$. Rotation of the η^2-bonded allene fragment followed by migration of the molybdenum-bonded hydrogen onto the central carbon atom of the co-ordinated allene would afford a 16-electron σ-bonded allyl species, which would be expected [19] to collapse to the isolated η^3-allyl complexes.

In the reactions of the unsymmetrical acetylene (MeC_2R) complexes (R = Et or Pr^i) it is interesting to note that there

---

* This is so since C(3) is further from the MoCP plane than C(1) by 0.269 Å, the C(1) · · · C(3) distance is 2.448 Å, and $\tan^{-1}(0.269/2.448) = 6.3°$.

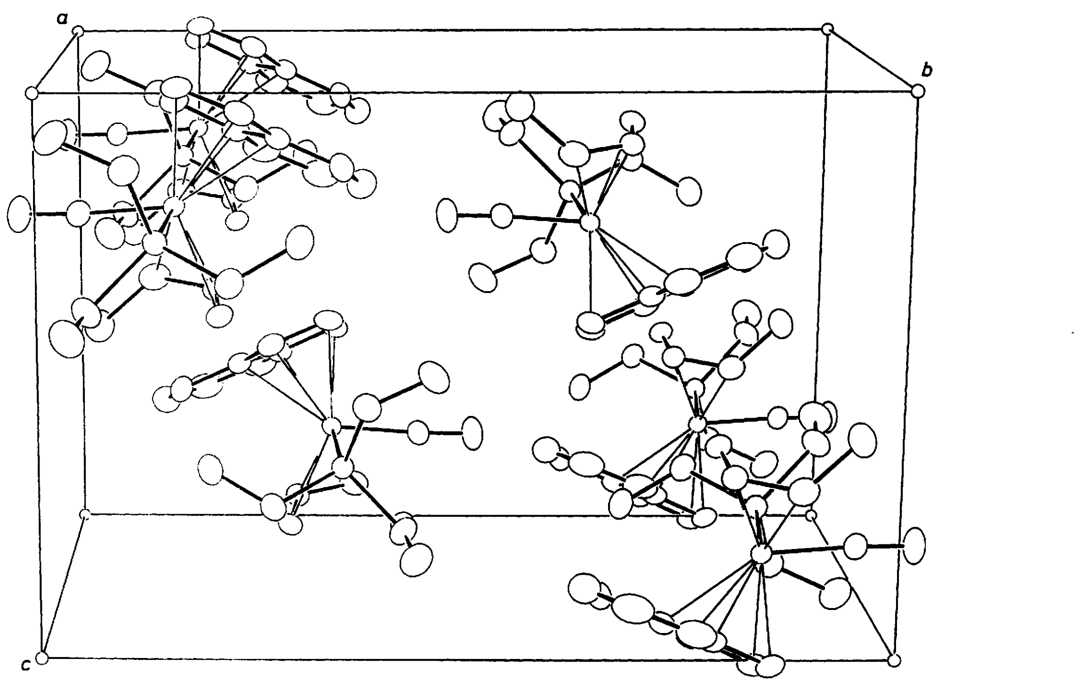

Figure 2. Crystal packing diagram of (7), with hydrogen atoms omitted. The unit-cell origin is in the top left-hand corner

was no evidence for the formation of complexes containing the allylic fragments η^3-CHMe$\cdots$CH$\cdots$CHMe or η^3-CMe$_2\cdots$CH$\cdots$CHMe, indicating a high degree of regiocontrol. Since hydrogen migration from the molybdenum to a carbon of the co-ordinated acetylene would be expected to be reversible it is possible that this selectivity arises because of the reactivity sequence $CH_3 > CH_2CH_3 > CH(CH_3)_2$ with regard to β-hydrogen elimination.

In the reactions leading to the formation of the unsymmetrical complexes (6) and (7), it is noteworthy that the predominant products are those with the triethylphosphine ligand *trans* to the *anti*-methyl substituent of the η^3-allyl system. This would suggest that β-hydrogen elimination occurs faster from a position *trans* to the PEt_3 ligand compared with the same reaction *trans* to CO. This point is illustrated in Scheme 1 by noting the positions of the $P(OMe)_3$ ligand L*.

In this proposed reaction scheme the postulated σ-vinyl intermediates have a pivotal role, and it was clearly important to provide support for their involvement. This was provided by examining the reaction of hydride anion sources with [Mo{P(OMe)$_3$}$_2$(η-HC$_2$Bu^t)(η-C$_5$H$_5$)][BF$_4$] in the presence of excess trimethyl phosphite. The product of the reaction (8) was obtained as a yellow crystalline material, which on the basis of elemental analysis and n.m.r. spectra (see Experimental section) could be formulated as a tris(phosphite)-vinyl species with molecular formula [Mo{P(OMe)$_3$}$_3${σ-(*E*)-CH=CHBu^t}(η-C$_5$H$_5$)]. The corresponding reaction with NaBD$_4$ afforded [Mo{P(OMe)$_3$}$_2${σ-(*E*)-CH=CDBu^t}(η-C$_5$H$_5$)]. In order to define precisely the structure of (8), in particular the stereochemistry of the σ-vinyl ligand, a single-crystal *X*-ray diffraction study was carried out, and bond lengths, interbond angles and atomic positional parameters are listed in Tables 7, 8, and 9 respectively.

The molecular structure of (8) is illustrated in Figures 3 and 4, and is of the familiar [20] ' piano stool ' type [ML$_4$(η-C$_5$H$_5$)]. The vinyl ligand σ-bound to the molybdenum atom forms one of the four legs of the piano-stool, and has an (*E*)-stereochemistry. This conformation of the vinyl ligand allows minimisation of steric interaction between the tertiary butyl

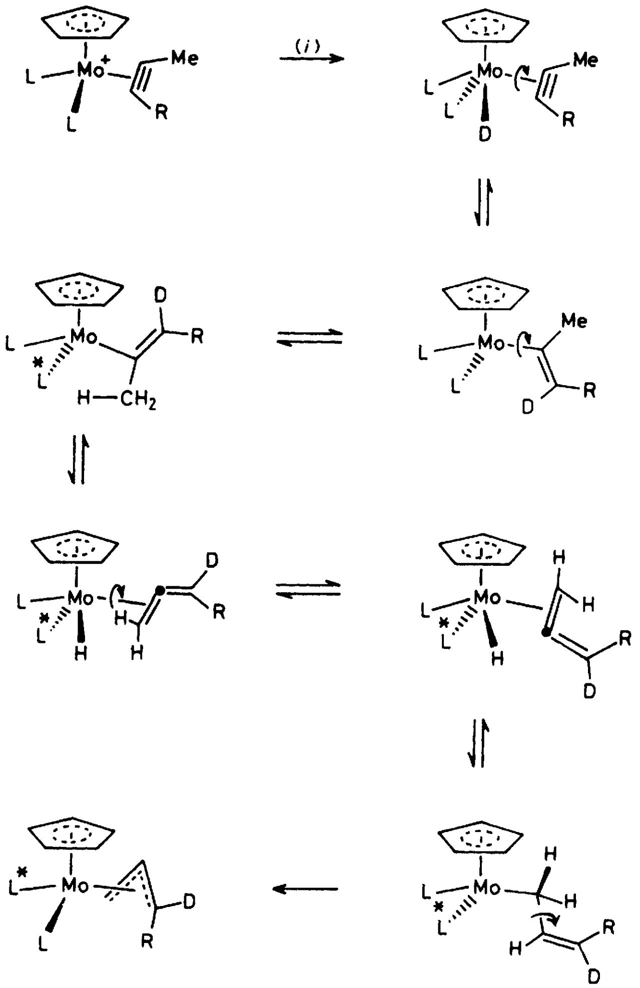

Scheme 1. L = P(OMe)$_3$; R = Me, Et, or Pr^i; (*i*) BH$_4^-$, BHBu$^s{}_3^-$, or BD$_4^-$. Formation of the D derivative is the example shown

Table 7. Bond lengths (Å) for $[\mathrm{Mo\{P(OMe)_3\}_3\{\sigma\text{-}(\mathit{E})\text{-}CH{=}CHBu^t\}(\eta\text{-}C_5H_5)}]$ (8) *

Mo–P(1)	2.352(1)	Mo–P(2)	2.367(1)
Mo–P(3)	2.359(1)	Mo–C(10)	2.243(2)
Mo–C(16)	2.370(2)	Mo–C(17)	2.340(2)
Mo–C(18)	2.307(2)	Mo–C(19)	2.323(2)
Mo–C(20)	2.356(2)	P(1)–O(1)	1.634(1)
P(1)–O(2)	1.599(1)	P(1)–O(3)	1.624(1)
P(2)–O(4)	1.619(1)	P(2)–O(5)	1.629(1)
P(2)–O(6)	1.606(1)	P(3)–O(7)	1.640(1)
P(3)–O(8)	1.606(1)	P(3)–O(9)	1.620(1)
O(1)–C(1)	1.429(2)	O(2)–C(2)	1.425(2)
O(3)–C(3)	1.437(2)	O(4)–C(4)	1.436(3)
O(5)–C(5)	1.431(3)	O(6)–C(6)	1.432(3)
O(7)–C(7)	1.430(3)	O(8)–C(8)	1.411(2)
O(9)–C(9)	1.441(2)	C(10)–C(11)	1.336(3)
C(11)–C(12)	1.518(3)	C(12)–C(13)	1.527(3)
C(12)–C(14)	1.531(3)	C(12)–C(15)	1.531(3)
C(16)–C(17)	1.406(3)	C(16)–C(20)	1.411(3)
C(17)–C(18)	1.414(3)	C(18)–C(19)	1.413(3)
C(19)–C(20)	1.412(3)	C(10)–H(10)	0.96(2)
C(11)–H(11)	1.02(2)		

* All other C–H distances were fixed at 0.96 Å.

Table 8. Interbond angles (°) for $[\mathrm{Mo\{P(OMe)_3\}_3\{\sigma\text{-}(\mathit{E})\text{-}CH{=}CHBu^t\}(\eta\text{-}C_5H_5)}]$ (8) *

P(1)–Mo–P(2)	80.6(1)	P(1)–Mo–P(3)	81.5(1)
P(2)–Mo–P(3)	117.1(1)	P(1)–Mo–C(10)	127.1(1)
P(2)–Mo–C(10)	74.1(1)	P(3)–Mo–C(10)	70.5(1)
P(1)–Mo–C(16)	114.0(1)	P(2)–Mo–C(16)	90.3(1)
P(3)–Mo–C(16)	151.0(1)	C(10)–Mo–C(16)	111.8(1)
P(1)–Mo–C(17)	146.8(1)	P(2)–Mo–C(17)	104.3(1)
P(3)–Mo–C(17)	122.0(1)	C(10)–Mo–C(17)	85.1(1)
C(16)–Mo–C(17)	34.7(1)	P(1)–Mo–C(18)	133.4(1)
P(2)–Mo–C(18)	139.4(1)	P(3)–Mo–C(18)	92.9(1)
C(10)–Mo–C(18)	93.0(1)	C(16)–Mo–C(18)	58.5(1)
C(17)–Mo–C(18)	35.4(1)	P(1)–Mo–C(19)	98.8(1)
P(2)–Mo–C(19)	145.9(1)	P(3)–Mo–C(19)	96.3(1)
C(10)–Mo–C(19)	127.5(1)	C(16)–Mo–C(19)	58.5(1)
C(17)–Mo–C(19)	58.7(1)	C(18)–Mo–C(19)	35.5(1)
P(1)–Mo–C(20)	89.4(1)	P(2)–Mo–C(20)	111.1(1)
P(3)–Mo–C(20)	128.5(1)	C(10)–Mo–C(20)	143.0(1)
C(16)–Mo–C(20)	34.7(1)	C(17)–Mo–C(20)	57.9(1)
C(18)–Mo–C(20)	58.5(1)	C(19)–Mo–C(20)	35.1(1)
Mo–P(1)–O(1)	123.1(1)	Mo–P(1)–O(2)	119.2(1)
O(1)–P(1)–O(2)	96.7(1)	Mo–P(1)–O(3)	111.1(1)
O(1)–P(1)–O(3)	99.9(1)	O(2)–P(1)–O(3)	103.5(1)
Mo–P(2)–O(4)	111.2(1)	Mo–P(2)–O(5)	122.0(1)
O(4)–P(2)–O(5)	100.1(1)	Mo–P(2)–O(6)	120.0(1)
O(4)–P(2)–O(6)	104.6(1)	O(5)–P(2)–O(6)	95.7(1)
Mo–P(3)–O(7)	122.1(1)	Mo–P(3)–O(8)	125.2(1)
O(7)–P(3)–O(8)	95.0(1)	Mo–P(3)–O(9)	110.9(1)
O(7)–P(3)–O(9)	99.5(1)	O(8)–P(3)–O(9)	99.2(1)
P(1)–O(1)–C(1)	118.2(1)	P(1)–O(2)–C(2)	129.4(1)
P(1)–O(3)–C(3)	120.6(1)	P(2)–O(4)–C(4)	121.7(1)
P(2)–O(5)–C(5)	119.0(1)	P(2)–O(6)–C(6)	127.5(1)
P(3)–O(7)–C(7)	120.1(1)	P(3)–O(8)–C(8)	125.1(1)
P(3)–O(9)–C(9)	121.2(1)	Mo–C(10)–C(11)	128.2(1)
C(10)–C(11)–C(12)	128.1(2)	C(11)–C(12)–C(13)	113.1(2)
C(11)–C(12)–C(14)	108.5(2)	C(13)–C(12)–C(14)	109.2(2)
C(11)–C(12)–C(15)	108.4(2)	C(13)–C(12)–C(15)	108.5(2)
C(14)–C(12)–C(15)	108.9(2)	Mo–C(16)–C(17)	71.5(1)
Mo–C(16)–C(20)	72.1(1)	C(17)–C(16)–C(20)	107.7(2)
Mo–C(17)–C(16)	73.8(1)	Mo–C(17)–C(18)	71.0(1)
C(16)–C(17)–C(18)	108.3(2)	Mo–C(18)–C(17)	73.6(1)
Mo–C(18)–C(19)	72.8(1)	C(17)–C(18)–C(19)	107.9(2)
Mo–C(19)–C(18)	71.6(1)	Mo–C(19)–C(20)	73.7(1)
C(18)–C(19)–C(20)	107.5(2)	Mo–C(20)–C(16)	73.1(1)
Mo–C(20)–C(19)	71.1(1)	C(16)–C(20)–C(19)	108.5(2)
Mo–C(10)–H(10)	118.6(12)	C(11)–C(10)–H(10)	113.1(12)
C(10)–C(11)–H(11)	121.9(14)	C(12)–C(11)–H(11)	110.0(14)

* All other hydrogen atom geometries were constrained as described in the text.

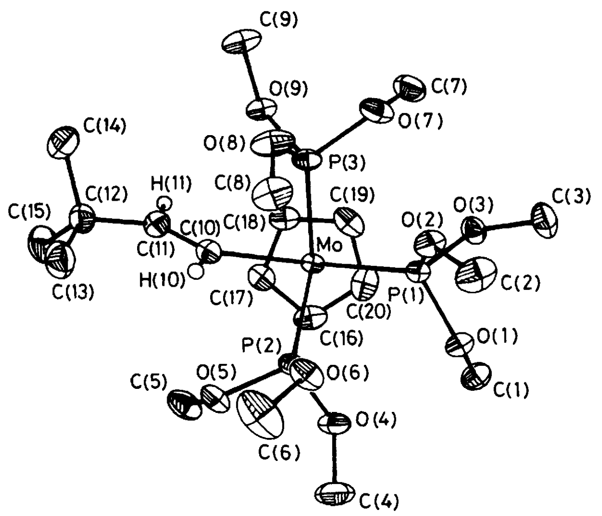

Figure 3. Molecular structure for $[\mathrm{Mo\{P(OMe)_3\}_3\{\sigma\text{-}(\mathit{E})\text{-}CH{=}CHBu^t\}(\eta\text{-}C_5H_5)}]$ (8) with thermal ellipsoids drawn as for Figure 1

substituent and the cyclopentadienyl ring. The planarity of the vinyl ligand at C(10) and C(11) is reflected in their bond angles summing to 359.9 and 360.0° respectively. The Mo–C(vinyl) bond length [2.243(2) Å] is at the low end of the range observed for formally Mo–C(σ) single bonds in related compounds: for example, $[\mathrm{Mo\{\sigma\text{-}C(CN)_2C(CN)_2Me\}(CO)_2(PPh_3)(\eta^5\text{-}C_5H_5)}]$ [21] 2.414(4) Å, $[\mathrm{Mo(Et)(CO)_3(\eta^5\text{-}C_5H_5)}]$ [22] 2.397(19) Å, $[\mathrm{Mo(C_6F_5)(CO)_2(\eta\text{-}C_7H_7)}]$ [23] 2.244(9) Å, $[\mathrm{Mo\text{-}C(O)\text{-}CH_2CH_2NH_2(CO)_2(\eta^5\text{-}C_5H_5)}]$ [24] 2.22(2) Å, and it is close to that observed for the only other molybdenum vinyl complex of this type $[\mathrm{Mo\{C(CF_3){=}C(CF_3)C_5H_5\}(CF_3C_2CF_3)(\eta^5\text{-}C_5H_5)}]$ [25] [2.251(9) Å]. This bond distance therefore implies some π contribution to Mo–vinyl bonding *via* interaction of filled orbitals on the metal and the π* orbitals on the vinyl ligand. This interaction is, however, not as strong as in the case of formal Mo=C double bonds as, for example, in $[\mathrm{Mo\{C(OEt)Ph\}(GePh_3)(CO)_2(\eta\text{-}C_5H_5)}]$,[26] Mo–C 2.062(11) Å, $[\mathrm{Mo(CNPh)I(CO)_2(\eta\text{-}C_5H_5)}]$,[27] Mo–C 2.025(10) Å, and $[\mathrm{Mo\{C(CH_2Bu^t)P(O)\}(OMe)_2I\{P(OMe)_3\}(\eta\text{-}C_5H_5)}]$ [28] 2.006(4) Å; and produces no significant lengthening of the C=C double bond [C(10)–C(11) 1.336(3) Å], although this is not surprising (*cf.* the very small changes observed in C≡O bond length on co-ordination of carbon monoxide).

The orientational preferences of carbene and vinylidene ligands bonded to $\mathrm{ML_2(\eta\text{-}C_5H_5)}$ fragments have been analysed [29] and found to be electronically determined, the conformation in which the ligand π-acceptor orbitals lie parallel to the plane of the cyclopentadienyl ligand being preferred. In the case of such ligands bonding to a $\mathrm{ML_3(\eta\text{-}C_5H_5)}$ fragment, although similar electronic factors hold, the structural evidence shows a less clear-cut distinction; for example, in $[\mathrm{Mo\{C(OEt)Ph\}(GePh_3)(CO)_2(\eta\text{-}C_5H_5)}]$ and $[\mathrm{Mo\{C{=}C(CN)_2\}I(CO)_2(\eta\text{-}C_5H_5)}]$ the best π-acceptor orbitals lie parallel and perpendicular to the $\eta\text{-}\mathrm{C_5H_5}$ plane respectively. In the case of the vinyl ligand in (8) these acceptor orbitals (π* with respect

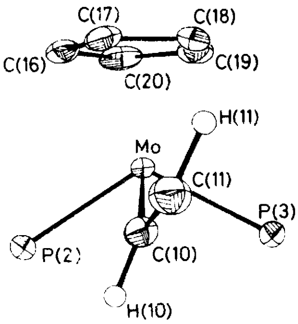

Figure 4. Alternative view of complex (8) showing the orientation of the σ-vinyl ligand

to C–C bonding) are slightly twisted with respect to the conformation observed for [Mo{C(OEt)Ph}(GePh$_3$)(CO)$_2$(η-C$_5$H$_5$)], so that the MoC(10)C(11)C(12) plane makes an angle of 68.8° with the η-C$_5$H$_5$ plane (*cf. ca.* 90° in the carbene complex). This twisting is probably due to steric (crystal packing) effects and reflects the low barrier to rotation about the Mo–C bond. This is in accord with the temperature invariant (183—293 K) ^{31}P n.m.r. spectrum of (8), which appeared as an AB$_2$ spin system, implying time-averaged molecular C_s symmetry in solution. The phosphorus *transoid* to the vinyl ligand shows the shortest Mo–P distance 2.352(1) Å [*cf.* average Mo–P(*cisoid*) 2.363(2) Å]. The interligand angles in the basal plane are in the usual range for ML$_4$(η-C$_5$H$_5$) complexes showing the expected distortions due to the smaller bulk of the vinyl ligand relative to the phosphite ligands: *transoid* angles are P(1)–Mo–C(10) 127.1(1)°, P(2)–Mo–P(3) 117.1(1)°; *cisoid* angles P(1)–Mo–P(2) 80.6(1)°, P(1)–Mo–P(3) 81.5(1)°, C(10)–Mo–P(2) 74.1(1)°, C(10)–Mo–P(3) 70.5(1)°. The remaining molecular parameters are unremarkable.

Thus the formation of the complex (8) and its deuterium-substituted analogue is consistent with a reaction path which involves attack by hydride on the molybdenum to generate an 18-electron species where the hydrido and 3,3-dimethylbut-1-yne ligands have a relative *cis*-configuration. Rotation of the acetylene followed by *cis*-coplanar H-migration can lead to the formation of the two illustrated (Scheme 2) isomeric 16-electron σ-bonded vinyl species, where thermodynamic control would be expected to favour the isomer with the bulky Bu^t group remote from the metal. Unlike the methyl-substituted acetylenes this intermediate does not have available a β-elimination reaction pathway, therefore simple capture by trimethyl phosphite occurs to form the isolated tris-phosphite complex.

The reaction of [Mo{P(OMe)$_3$}$_2$(η-HC$_2$Pr^i)(η-C$_5$H$_5$)][BF$_4$] with a source of H$^-$ in the presence of P(OMe)$_3$ was next examined in the belief that an analogue of (8) would be formed. However, reaction with K[BHBu$^s_3$] at −78 °C in thf afforded in good yield a yellow crystalline allylic complex (9) with molecular formula [Mo{P(OMe)$_3$}$_2$(η^3-CH$_2$⋯CH⋯CMe$_2$)(η-C$_5$H$_5$)], identified by elemental analysis and n.m.r. spectroscopy. The ^{13}C-{^{1}H} n.m.r. spectrum (Table 2) showed typical η^3-allylic signals at 67.4 p.p.m. (central C), 63.2 p.p.m. (substituted C), and 25.6 p.p.m. (unsubstituted C) together with two methyl signals at 31.4 and 24.9 p.p.m. The 6 p.p.m. separation of the methyl signals, the low-field shift of the substituted terminal allylic carbon, together with the fact that it did not carry a proton substituent (^{13}C off-resonance and ^{1}H decoupled spectrum), indicated that the allyl complex was the 1,1-dimethyl substituted isomer. This was confirmed by the ^{1}H n.m.r., which showed three signals of equal intensity at 3.76 p.p.m. (H$_c$), 2.08 p.p.m. (H$_s$) and 1.50 p.p.m. (H$_a$). In addition there were two methyl singlets at 1.91 (Me$_{s'}$) and 1.23 p.p.m. (Me$_{a'}$).

When Li[BDEt$_3$] was used as a source of D$^-$, the deuterium-substituted analogue of the complex (9) was formed in which the deuterium exclusively occupied the *syn*-position on the allyl fragment. The central proton was reduced to a doublet [*J*(HH) 9.0 Hz], and the signal at 2.06 p.p.m. was absent. Reaction of the cation [Mo{P(OMe)$_3$}$_2$(DC$_2$Pr^i)(η-C$_5$H$_5$)]$^+$ with K[BHBu$^s_3$] afforded the deuterium-substituted complex (9), where the deuterium was in the position formerly occupied by H$_a$, the signal at 1.50 p.p.m. being absent and that of H$_c$ being reduced to a doublet [*J*(HH) 7.5 Hz].

As is shown in Scheme 3 these observations, including the deuterium labelling experiments, are fully consistent with the previously suggested reaction path for the formation of allyl complexes, if it is assumed that an initially formed hydrido(3-methylbut-1-yne) complex can reversibly transform into the two illustrated isomeric 16-electron σ-vinyl complexes. Then the thermodynamically less stable isomer, in which the isopropyl group is attached to the α-carbon atom, can undergo a β-hydrogen elimination reaction to form (9).

These results with unsymmetrical acetylene cations require that access be gained to 18-electron hydrido(acetylene) intermediates. Although we tend to favour the idea that these

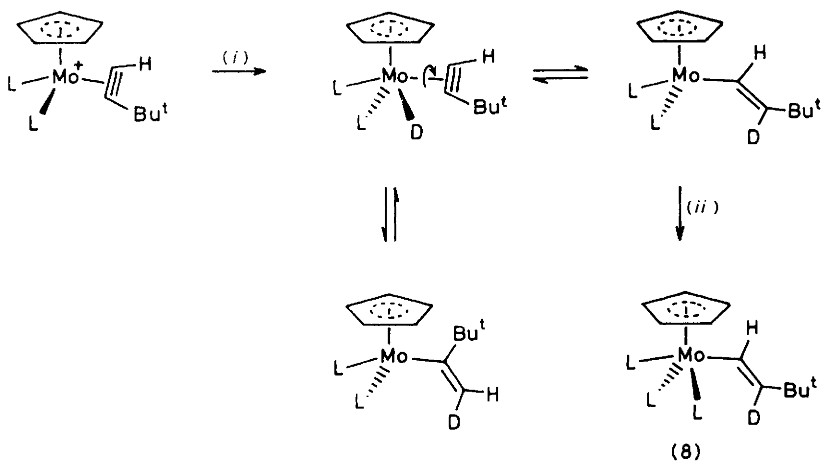

Scheme 2. L = P(OMe)$_3$; (*i*) BH$_4^-$, BHBu$^s_3{}^-$, or BDEt$_3{}^-$; (*ii*) + L. Formation of the D derivative is the example shown

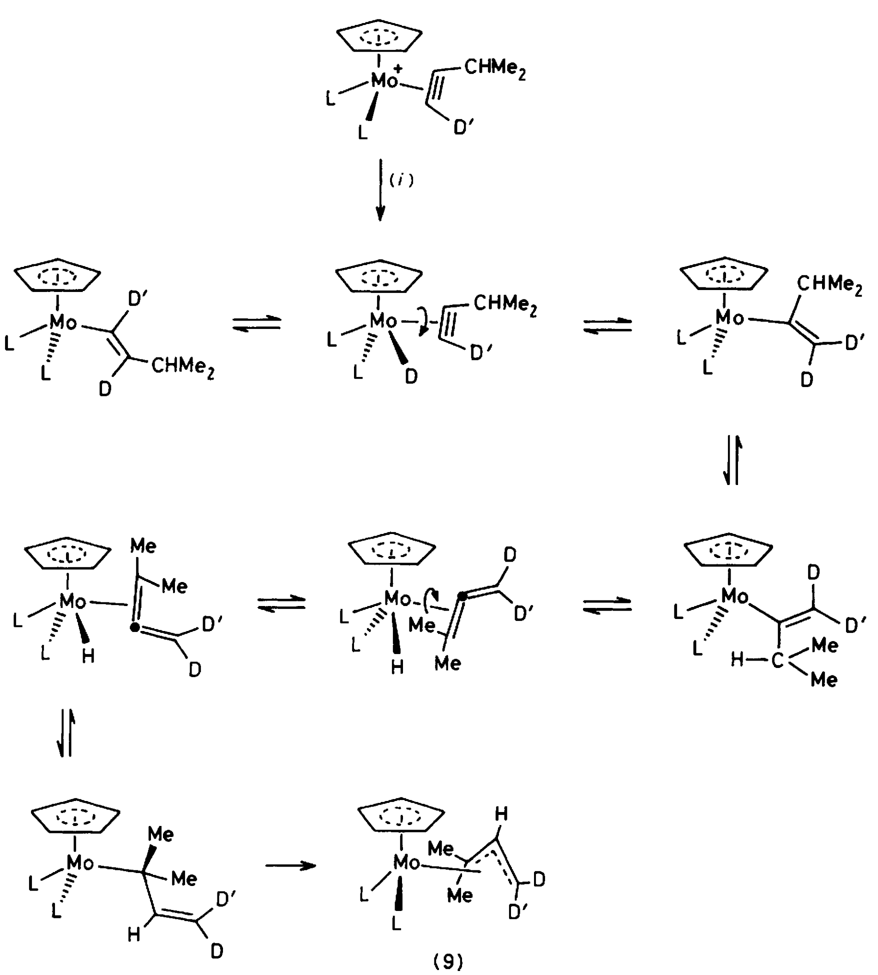

Scheme 3. L = P(OMe)$_3$; (*i*) BHBu$^s_3$$^-$ or BDEt$_3$$^-$. Formation of the D derivative is the example shown

species are generated directly by nucleophilic attack on molybdenum there is the interesting possibility that (3e) η^2-bonded cyclic alkylidene or metallacyclopropenes are involved in their formation. As is illustrated in Scheme 4, metallacyclopropenes can in principle be formed in one step by nucleophilic attack on the *substituted* carbon of a (4e) η^2-bonded acetylene or by collapse [(1e) σ to (3e) η^2] of a (1e) σ-bonded vinyl complex formed by *trans* attack on the substituted carbon. Thus, metallacyclopropenes can provide a reaction path for *E* to *Z* isomerisation of co-ordinatively unsaturated σ-vinyl species, and access can be gained *via* a β-vinylic elimination to a hydrido(acetylene) complex. Support for this idea derives from our observation[30] that K[BHBu$^s_3$] reacts with [Mo{P(OMe)$_3$}$_2$(η-PhC$_2$Ph)(η-C$_5$H$_5$)][BF$_4$] to form a stable crystalline (3e) η^2-bonded cyclic alkylidene complex [Mo{=C(Ph)CHPh}{P(OMe)$_3$}$_2$(η-C$_5$H$_5$)] structurally identified by *X*-ray crystallography. This suggestion will be explored in detail in a subsequent paper.

Experimental

The instrumentation used and techniques employed were as previously described.[1]

Reaction of NaBH$_4$ *with* [Mo(CO)(PEt$_3$)(η-MeC$_2$Me)(η^5-C$_9$H$_7$)][BF$_4$].—An excess of NaBH$_4$ (0.1 g, 2.6 mmol) was added at room temperature to a stirred suspension of [Mo(CO)(PEt$_3$)(η-MeC$_2$Me)(η^5-C$_9$H$_7$)][BF$_4$][8] (1.0 g, 2.0 mmol) in thf (20 cm^3) to which triethylphosphine (0.2 cm^3) had been added. After 1 h at room temperature a clear maroon solution was formed. The volatile material was removed *in vacuo*, the dark red solid extracted with diethyl ether, and the resultant solution filtered through a pad (2 cm) of dry Kieselguhr. The diethyl ether was removed *in vacuo*, and the oil held under vacuum for 3 h in the presence of a dry-ice cooled cold finger in order to remove the excess triethylphosphine, which collected on the cold finger as a white solid. The resulting dark residue was extracted with diethyl ether–hexane (1 : 10, 4 × 5 cm^3) and purified by column chromatography on an alumina packed column. Elution with diethyl ether–hexane (1 : 1) afforded a red band, which on cooling (−78 °C overnight) gave red *crystals* of (7) (0.6 g, 50%), ν_{CO} (hexane) 1 826 cm^{-1}.

Reaction of K[BHBu$^s_3$] *with* [Mo(Ph$_2$PCH=CHPPh$_2$)(η-MeC$_2$Me)(η-C$_5$H$_5$)][BF$_4$].—The turquoise salt [Mo(Ph$_2$PCH=CHPPh$_2$)(η-MeC$_2$Me)(η-C$_5$H$_5$)] [BF$_4$][8] (0.7 g, 1.0 mmol) was suspended in thf (25 cm^3) and cooled to −78 °C. One equivalent of K[BHBu$^s_3$] (0.5 mol dm^{-3} solution in thf) was added dropwise to the stirred suspension and the reaction mixture allowed to warm to room temperature by which time it appeared as a dirty orange solution. The volatile material was removed *in vacuo* and the residue extracted with toluene; the solution was filtered through Kieselguhr. The volume of solvent was reduced *in vacuo* and the remainder introduced

Table 9. Fractional atomic co-ordinates for $[Mo\{P(OMe)_3\}_3\{\sigma\text{-}(E)\text{-}CH{=}CHBu^t\}(\eta\text{-}C_5H_5)]$ (8)

Atom	*x*	*y*	*z*	Atom	*x*	*y*	*z*
Mo	0.247 90(1)	0.222 67(1)	0.320 37(1)	H(8C)	0.312 2(2)	0.229 2(2)	0.500 30(10)
P(1)	0.288 19(3)	0.054 04(3)	0.364 27(2)	H(9A)	0.628 8(2)	0.440 1(2)	0.330 19(12)
P(2)	0.093 47(4)	0.202 81(3)	0.396 31(2)	H(9B)	0.644 3(2)	0.341 1(2)	0.378 69(12)
P(3)	0.428 87(4)	0.256 77(4)	0.374 69(2)	H(9C)	0.582 6(2)	0.440 4(2)	0.407 17(12)
O(1)	0.189 58(10)	−0.033 44(10)	0.376 82(6)	H(13A)	0.190 5(3)	0.620 7(2)	0.498 02(11)
O(2)	0.353 27(10)	0.041 46(10)	0.440 07(6)	H(13B)	0.238 5(3)	0.506 7(2)	0.504 83(11)
O(3)	0.368 02(11)	−0.010 25(10)	0.311 00(6)	H(13C)	0.119 3(3)	0.526 7(2)	0.466 54(11)
O(4)	−0.001 48(10)	0.123 26(11)	0.362 61(7)	H(14A)	0.360 2(2)	0.682 4(2)	0.439 32(13)
O(5)	0.012 18(11)	0.300 67(10)	0.416 73(7)	H(14B)	0.402 0(2)	0.628 4(2)	0.370 30(13)
O(6)	0.116 15(11)	0.162 68(11)	0.476 48(6)	H(14C)	0.414 9(2)	0.570 7(2)	0.443 61(13)
O(7)	0.532 97(11)	0.171 28(11)	0.374 16(7)	H(15A)	0.172 9(3)	0.710 4(2)	0.384 86(14)
O(8)	0.451 77(12)	0.290 22(13)	0.456 23(7)	H(15B)	0.097 9(3)	0.619 6(2)	0.352 25(14)
O(9)	0.490 19(10)	0.353 97(10)	0.336 48(6)	H(15C)	0.206 3(3)	0.657 5(2)	0.313 50(14)
C(1)	0.123 7(2)	−0.069 9(2)	0.316 31(10)	H(16)	0.039 4(2)	0.212 2(2)	0.223 77(9)
C(2)	0.335 3(2)	−0.032 6(2)	0.494 98(11)	H(17)	0.135 9(2)	0.388 9(15)	0.234 18(8)
C(3)	0.415 0(2)	−0.110 0(2)	0.331 44(12)	H(18)	0.348 4(2)	0.363 1(2)	0.219 31(9)
C(4)	−0.099 4(2)	0.092 8(3)	0.401 01(14)	H(19)	0.383 1(2)	0.169 4(2)	0.198 23(9)
C(5)	−0.039 2(2)	0.362 5(2)	0.360 78(12)	H(20)	0.191 8(2)	0.076 8(2)	0.201 01(9)
C(6)	0.065 1(3)	0.200 6(3)	0.539 31(11)	C(11)	0.259 2(2)	0.468 78(14)	0.361 46(9)
C(7)	0.579 6(2)	0.140 4(2)	0.308 37(12)	C(12)	0.248 6(2)	0.569 60(14)	0.403 18(10)
C(8)	0.385 2(2)	0.258 9(2)	0.513 24(10)	C(13)	0.194 8(3)	0.554 0(2)	0.474 97(11)
C(9)	0.594 6(2)	0.398 3(2)	0.365 96(12)	C(14)	0.367 7(2)	0.616 9(2)	0.415 06(13)
C(10)	0.240 67(14)	0.371 17(13)	0.383 35(8)	C(15)	0.174 3(3)	0.645 8(2)	0.358 96(14)
H(6A)	0.110 5(3)	0.177 4(3)	0.579 89(11)	C(16)	0.119 4(2)	0.225 5(2)	0.219 95(9)
H(6B)	−0.010 1(3)	0.171 3(3)	0.541 07(11)	C(17)	0.173 1(2)	0.323 5(15)	0.225 86(8)
H(6C)	0.060 2(3)	0.275 4(3)	0.539 66(11)	C(18)	0.291 3(2)	0.309 2(2)	0.217 45(9)
H(7A)	0.624 7(2)	0.086 8(2)	0.319 70(12)	C(19)	0.310 7(2)	0.201 7(2)	0.205 82(9)
H(7B)	0.616 6(2)	0.197 9(2)	0.286 05(12)	C(20)	0.204 3(2)	0.150 4(2)	0.207 40(9)
H(7C)	0.521 1(2)	0.112 7(2)	0.276 55(12)	H(10)	0.218(2)	0.368(2)	0.431 5(11)
H(8A)	0.374 9(2)	0.320 5(2)	0.541 29(10)	H(11)	0.286(3)	0.485(2)	0.311 9(12)
H(8B)	0.429 9(2)	0.208 9(2)	0.540 32(10)				

onto a short (4 × 10 cm) alumina packed column. Elution with toluene afforded an orange band, which was collected and reduced in volume to 10 cm^3. Hexane was added without mixing and the vessel cooled to −30 °C overnight, affording red *crystals* of (5) (0.4 g, 65%).

Similar procedures were used in the preparation of the related complexes (1), (2), (3), (4), and (6).

Reaction of $K[BHBu^s_3]$ *with* $[Mo\{P(OMe)_3\}_2(\eta\text{-}HC_2Bu^t)(\eta\text{-}C_5H_5)][BF_4]$.—An excess of $K[BHBu^s_3]$ (3.0 cm^3 of a 0.5 mol dm^{-3} solution in thf, 1.5 mmol) was added dropwise to a stirred suspension of $[Mo\{P(OMe)_3\}_2(\eta\text{-}HC_2Bu^t)(\eta\text{-}C_5H_5)][BF_4]$ (0.5 g, 0.86 mmol) in thf (30 cm^3) containing an excess of trimethyl phosphite (0.2 g, 1.6 mmol) and cooled to −60 °C. The reaction mixture was stirred for 30 min and then allowed to warm to −30 °C. The volatile material was removed *in vacuo* from the cold (−30 °C) reaction mixture, and the residue extracted with cold (−50 °C) hexane (20 cm^3) and filtered. The extract was cooled to −78 °C affording yellow *crystals* of (8) (0.36 g, 70%) (Found: C, 40.1; H, 7.1; *M*, 616. $C_{20}H_{43}MoO_9P_3$ requires C, 39.0; H, 7.0%; *M*, 616). N.m.r.: ^1H (C_6D_6, 303 K), δ 6.9 [m, 1 H, H^1, J_{12} 17, $J(H^1P_B)$ 14, $J(H^1P_A)$ 7], 5.6 [dt, 1 H, H^2, J_{12} 17, $J(H^2P_B)$ 2 Hz], 5.05 (s, 5 H, C_5H_5), 3.5 (m, 27 H, PO*Me*), 1.2 (s, 9 H, Bu^t); $^{13}C\text{-}\{^1H\}$ (thf, 303 K), δ 151.15 [t, MoCH=*C*HBu^t, $^3J(CP)$ 5.88], 129.19 [dt, Mo(*C*H=CHBu^t), $^2J(CP)$ 43.54, $^2J(CP)$ 5.13 Hz], 87.67 (s, C_5H_5), 51.61 (m, PO*Me*), 37.42 (s, *C*Me$_3$), 30.65 (s, C*Me*$_3$); $^{31}P\text{-}\{^1H\}$ (C_6D_6, 303 K), AB_2 spin system, δ_A 206.9, δ_B 193.6 p.p.m., $J(P_AP_B)$ 118.6 Hz.

A similar procedure was adopted in the corresponding reactions with $NaBH_4$ and $NaBD_4$ except that the reaction mixture was allowed to warm to room temperature before work-up. Yields of 45% were obtained.

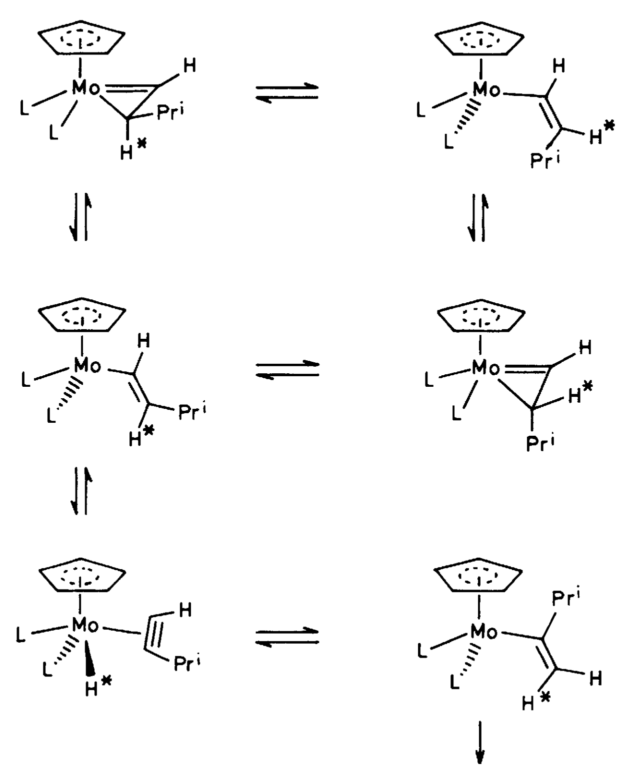

(9)

Scheme 4. L = $P(OMe)_3$; H* = hydride from $BHBu^s_3{}^-$

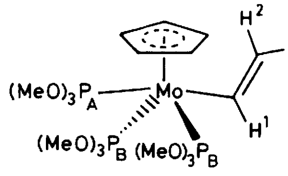

Crystal Structure Determinations of [Mo(CO)(PEt$_3$)(η^3-*anti*-1-MeC$_3$H$_4$)(η^5-C$_9$H$_7$)] (7) *and* [Mo{P(OMe)$_3$}$_3${σ-(*E*)-CH=CHBu^t}(η-C$_5$H$_5$)] (8).—*Collection and reduction of diffraction data.* A small dark red crystal of (7) (dimensions 0.3 × 0.2 × 0.2 mm), freshly crystallised from pentane, was sealed under N$_2$ in a thin-walled glass capillary [because solid (7) is air sensitive over days] for *X*-ray structure analysis. Diffraction measurements were made on a Nicolet P3m diffractometer after preliminary photographic examination of the crystal. Cell parameters were determined by least-squares fit to the setting angles of 15 centred reflections with $21 < 2\theta < 27°$. Intensity data were collected at room temperature for two unique octants of reciprocal space ($+h$, $+k$, $\pm l$) in the range $2.9 < 2\theta < 55.0°$. Reflections were scanned (θ—2θ mode) at a constant speed of 3.91° min^{-1} with scan width [2.0 + $\Delta(\alpha_2 - \alpha_1)$]° using graphite-monochromated Mo-K_α *X*-radiation (λ = 0.7107 Å). Analysis [31] of the intensities of three reflections remeasured after every 50 revealed no significant variation in crystal quality or experimental stability over the period of data collection. A total of 4 541 unique non-zero reflection intensities were measured; of these, 3 887 with $F_o^2 > 0.5\sigma(F_o^2)$ [where $\sigma(F_o^2)$ is the standard deviation in F_o based on counting statistics] were used in structure solution and refinement.

Crystal data for (7). C$_{19}$H$_{29}$MoOP, M = 400.4, Monoclinic, a = 10.038(2), b = 17.291(4), c = 11.346(3) Å, β = 95.000(18)°, U = 1 961.8(7) Å^3, Z = 4, D_c = 1.355 g cm^{-3}, $F(000)$ = 832, μ(Mo-K_α) = 6.7 cm^{-1}, space group $P2_1/n$ (alternative setting of $P2_1/c$, C^5_{2h}, no. 14).

A yellow crystal of (8) (dimensions 0.6 × 0.5 × 0.4 mm), grown from pentane solution at −30 °C, was sealed under N$_2$ in a thin-walled glass capillary [solid (8) is air sensitive over seconds] for *X*-ray structure analysis. The experimental procedure followed closely that for (7) differing only as specified below. All diffraction measurements were made at 195 K (maintained by locally modified Nicolet LT-1 apparatus). Fifteen reflections in the range $28 < 2\theta < 39°$ were used to derive cell parameters. Scan speeds in data collection varied between 2.0 and 58.6° min^{-1} depending on the intensity of an initial 2-s prescan; reflections with very low prescan intensities were not remeasured. Data were collected in the range $4 < 2\theta < 65°$ yielding 7 734 unique data of which 7 437 with $F_o^2 > 2\sigma(F_o^2)$ were used in structural determination and refinement. As for (7) no significant crystal decay or experimental instability was observed and no absorption nor extinction corrections were applied.

Crystal data for (8). C$_{20}$H$_{43}$MoO$_9$P$_3$, M = 616.4, Monoclinic, a = 11.731(3), b = 12.796(3), c = 18.827(4) Å, β = 92.33(2)°, U = 2 824(1) Å^3, Z = 4, D_c = 1.449 g cm^{-3}, $F(000)$ = 1 288, space group $P2_1/c$ (no. 14), μ(Mo-K_α) = 6.6 cm^{-1}.

Solution and refinement of the structures. Both structures were solved by conventional heavy-atom methods (Patterson and Fourier) and refined by least-squares methods [full matrix for (7) and blocked-cascade full matrix for (8)]. In both cases non-hydrogen atoms were refined without positional constraints and with anisotropic thermal parameters. For (7) non-methyl hydrogens of the allyl ligand were located on a difference electron-density map and refined without positional constraints; other hydrogen atoms were constrained to idealised geometries (all C–H 1.08 Å and H–C–H 109.5° for methylene and methyl hydrogens) riding in their respective carbon atoms. All hydrogen thermal parameters for (7) were fixed (at U = 0.10 Å^2 in methyl group, at 0.07 Å^2 for the remainder). Final residual indices for (7) were R = 0.0344, R' = 0.0459, and S = 1.62 with weights $w = [\{\sigma(F_o^2)/4F_o^2\} + 0.00159\ F_o^2]^{-1}$.* A final electron-density difference map showed no features >0.5 e Å^{-3}. Table 6 lists the derived atomic positional parameters (excepting those calculated for constrained H atoms which are in SUP 23528). Important bond lengths and interbond angles are listed in Tables 4 and 5.

For (8) all the hydrogen atoms were located on difference electron-density syntheses; the vinyl hydrogens were refined without constraints, all others being incorporated in the refined model as for (7) but with C–H bond lengths 0.96 Å and isotropic thermal parameters free to refine. Final residual indices were R = 0.026, R' = 0.026, and S = 1.33, with weights $w = [\{\sigma(F_o^2)/4F_o^2\} + 0.00015\ F_o^2]^{-1}$;* a final difference-Fourier synthesis showed no features of chemical significance (all <0.66 e A^{-3}). Fractional atomic co-ordinates are listed in Table 9 (excluding those H atoms constrained). Important bond lengths and interbond angles are given in Tables 7 and 8.

Complex neutral-atom scattering factors of ref. 32 were used throughout. Calculations on (7) were carried out on the University of London CDC 7600 computer using the SHELX 76 system of programs,[33] those in (8) using the SHELXTL programs on a Nicolet R3m/E structure determination system.

Acknowledgements

We thank the S.E.R.C. for financial support.

References

1 Part 26, Y. N. Al-Obaidi, M. Green, N. D. White, and G. E. Taylor, *J. Chem. Soc., Dalton Trans.*, 1982, 319.
2 O. Eisenstein and R. Hoffmann, *J. Am. Chem. Soc.*, 1981, **103**, 4308 and refs. therein.
3 M. H. Chisholm and H. C. Clark, *Acc. Chem. Res.*, 1973, **6**, 202.
4 D. L. Reger, C. J. Coleman, and P. J. McElligott, *J. Organomet. Chem.*, 1979, **171**, 73.
5 D. L. Reger and P. J. McElligott, *J. Am. Chem. Soc.*, 1980, **102**, 5923.
6 M. Bottrill and M. Green, *J. Am. Chem. Soc.*, 1977, **99**, 5795.
7 M. Bottrill and M. Green, *J. Chem. Soc., Dalton Trans.*, 1977, 2365.
8 S. R. Allen, P. K. Baker, S. G. Barnes, M. Green, L. Trollope, L. Manojlović-Muir, and K. W. Muir, *J. Chem. Soc., Dalton Trans.*, 1981, 873.
9 B. E. Schilling, R. Hoffmann, and J. W. Faller, *J. Am. Chem. Soc.*, 1979, **101**, 592.
10 J. W. Faller, C. C. Chen, M. J. Mattina, and A. Jakubowski, *J. Organomet. Chem.*, 1973, **52**, 361.
11 J. Collin, U. Charrier, M. J. Pouet, P. Cadiot, and J. L. Roustan, *J. Organomet. Chem.*, 1979, **168**, 321.
12 (*a*) F. A. Cotton and M. D. LaPrade, *J. Am. Chem. Soc.*, 1968, **90**, 5418; (*b*) M. Green, J. Z. Nyathi, C. Scott, F. G. A. Stone, A. J. Welch, and P. Woodward, *J. Chem. Soc., Dalton Trans.*, 1978, 1067; (*c*) G. Huttner, H. H. Britzinger, L. G. Bell, P. Fridrich, V. Bejenke, and D. Nengebaner, *J. Organomet. Chem.*, 1978, **145**, 329; (*d*) J. W. Faller, D. F. Chodosh, and D. Katahiva, *J. Organomet. Chem.*, 1980, **187**, 227; (*e*) D. S. Gill, P. K. Baker, M. Green, K. E. Paddick, M. Murray, and A. J. Welch, *J. Chem. Soc., Chem. Commun.*, 1981, 986.
13 (*a*) F. S. Stephens, *J. Chem. Soc., Dalton Trans.*, 1974, 13; (*b*) J. L. Atwood, W. E. Hunter, D. C. Honcir, E. Samuel, H.

---

* $R = [\Sigma|F_o - |F_c||/\Sigma|F_o|]$; $R' = [\Sigma w|F_o - |F_c||^2/\Sigma w|F_o|^2]^{\frac{1}{2}}$; $S - [\Sigma w|F_o - |F_c||^2/NO-NV]^{\frac{1}{2}}$.

Alt, and M. D. Rausch, *Inorg. Chem.*, 1975, **14**, 1757; (*c*) M. B. Herman, J. L. Atwood, I. Bernal, and W. A. Hermann, *J. Organomet. Chem.*, 1979, **179**, 403; (*d*) P. Caddy, M. Green, E. O'Brien, L. E. Smart, and P. Woodward, *J. Chem. Soc., Dalton Trans.*, 1980, 962; (*e*) Y. N. Al-Obaidi, M. Green, N. D. White, J.-M. Bassett, and A. J. Welch, *J. Chem. Soc., Chem. Commun.*, 1981, 494.

14 P. Caddy, M. Green, E. O'Brien, L. E. Smart, and P. Woodward, *Angew. Chem., Int. Ed. Engl.*, 1977, **16**, 648.

15 See, for example, F. A. Cotton and J. Takatts, *J. Am. Chem. Soc.*, 1968, **90**, 2031; F. Dawans, J. Dewailly, J. Meunier-Piret, and P. Piret, *J. Organomet. Chem.*, 1974, **76**, 53.

16 A. E. Smith, *Acta Crystallogr.*, 1965, **18**, 331.

17 B. C. Ward and J. L. Templeton, *J. Am. Chem. Soc.*, 1980, **102**, 1532; L. Ricard, R. Weiss, W. E. Newtom, G. J. J. Chen, and J. W. McDonald, *J. Am. Chem. Soc.*, 1978, **100**, 1318.

18 J. Schwartz, D. W. Hart, and B. McGiffert, *J. Am. Chem. Soc.*, 1974, **96**, 5613.

19 D. L. Thorn and R. Hoffmann, *J. Am. Chem. Soc.*, 1978, **100**, 2079.

20 P. Kubacek, R. Hoffmann, and Z. Haules, *Organometallics*, 1982, **1**, 180.

21 M. R. Churchill and S. W.-Y. Chang, *Inorg. Chem.*, 1975, **14**, 98.

22 M. J. Bennett and R. Mason, *Proc. Chem. Soc. London*, 1963, 273.

23 M. R. Churchill and T. A. O'Brien, *J. Chem. Soc. A*, 1969, 1110.

24 H. M. M. Shearer and J. D. Sowenby, *J. Chem. Soc., Dalton Trans.*, 1973, 2629.

25 J. L. Davidson, M. Green, F. G. A. Stone, and A. J. Welch, *J. Chem. Soc., Dalton Trans.*, 1977, 287.

26 J. Y. Y. Chan, W. K. Dean, and W. A. Graham, *Inorg. Chem.*, 1977, **16**, 1067.

27 G. A. Sim, J. G. Sime, D. I. Woodhouse, and G. R. Knox, *Acta Crystallogr., Sect. B*, 1979, **35**, 2406.

28 P. K. Baker, G. K. Barker, M. Green, and A. J. Welch, *J. Am. Chem. Soc.*, 1980, **102**, 7812.

29 B. E. R. Schilling, R. Hoffmann, and D. L. Lichtenberger, *J. Am. Chem. Soc.*, 1979, **101**, 585.

30 M. Green, N. C. Norman, and A. G. Orpen, *J. Am. Chem. Soc.*, 1981, **103**, 1267.

31 A. G. Modinos, DRSYN, a Fortran Program for Data Analysis, University of Bristol, 1973.

32 'International Tables for *X*-Ray Crystallography,' Kynoch Press, Birmingham, 1974, vol. 4, pp. 99—101.

33 SHELX, G. M. Sheldrick, University of Cambridge, 1976.

Received 9th July 1982; Paper 2/1164